Schweizerische Eidgenossenschaft
Confédération suisse
Confederazione Svizzera
Confederaziun svizra

Federal Department of the Environment, Transport, Energy and Communications DETEC

Swiss Federal Office of Energy SFOE
Energy Research and Cleantech Division

Final report (June 2022)

Flash-GT

Investigation of flame flashback at gas turbine relevant conditions through experiment and modelling

---

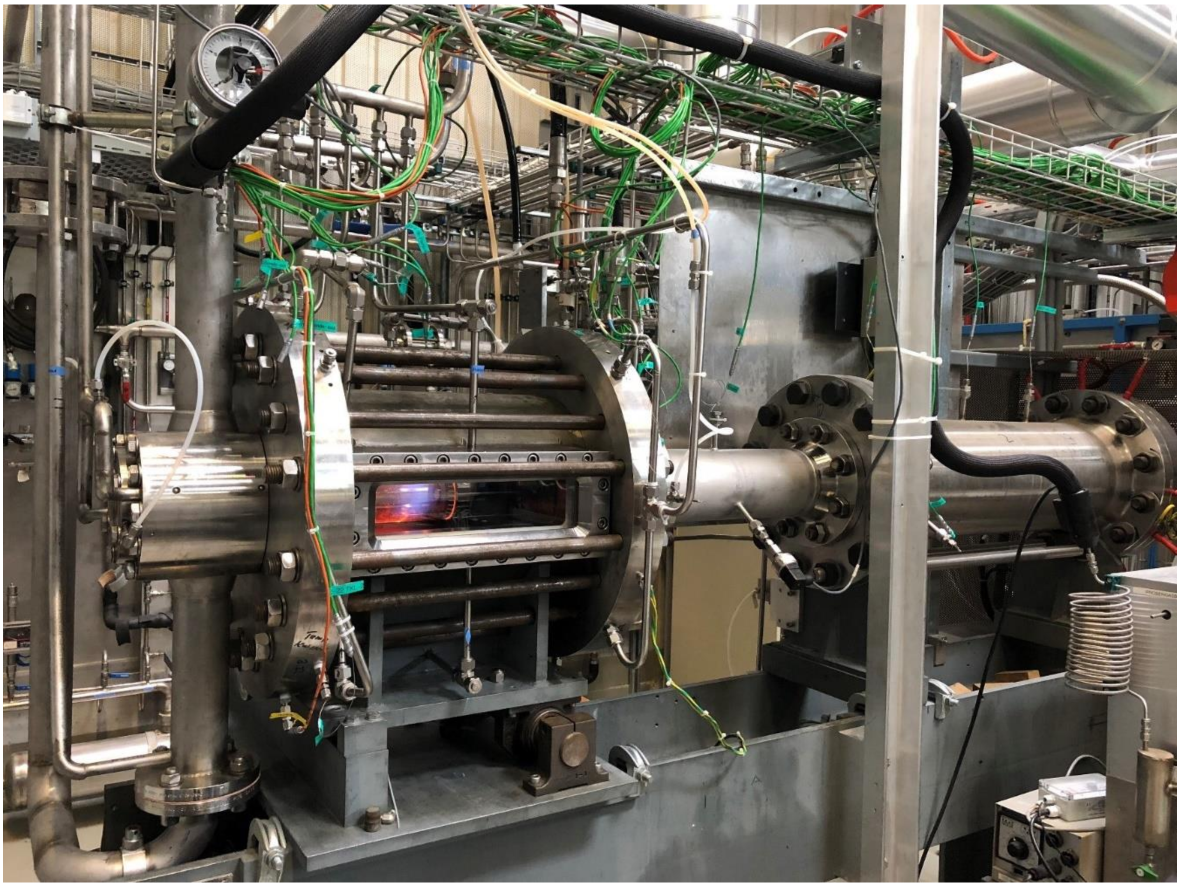

Source: © Ebi 2018

PAUL SCHERRER INSTITUT

Date: 30.06.2022

Location: Bern

Publisher:
Swiss Federal Office of Energy SFOE
Energy Research and Cleantech
CH-3003 Bern
www.bfe.admin.ch

Subsidy recipients:
Paul Scherrer Institut
Forschungsstrasse 111, 5232 Villigen PSI
www.psi.ch

Authors:
Dominik Ebi, PSI, dominik.ebi@psi.ch
Peter Jansohn, PSI, peter.jansohn@psi.ch
Alex Novoselov, ETHZ, agn@ethz.ch

SFOE project coordinators:
Carina Alles, carina.alles@bfe.admin.ch
Stephan Renz, info@renzconsulting.ch

SFOE contract number: SI/501821-01

Zusammenfassung

Gasturbinen bieten eine hohe Zuverlässigkeit in Verbindung mit einer hervorragenden Lastfolgefähigkeit - Eigenschaften, die in zukünftigen Energiesystemen immer wichtiger werden. Darüber hinaus erlaubt die magere Vormischverbrennung in Gasturbinen im Vergleich zur Verbrennung flüssiger oder fester Brennstoffe bemerkenswert niedrige Emissionen. Die derzeitige Generation von Brennern wurde aber hauptsächlich für den Betrieb mit Erdgas entwickelt und ist in Bezug auf das Brennstoff-Luft-Verhältnis auf enge Betriebsfenster beschränkt. Diese Brenner stehen nun vor der Herausforderung, in Gasturbinen mit alternativen, erneuerbaren Brenngasen betrieben zu werden, die in der Regel größere Anteile an Wasserstoff enthalten. Ein zentrales technisches Problem bei der Verbrennung von Brenngasen mit hohem Wasserstoffanteil ist die Vermeidung eines Flammenrückschlags in den Vormischbereich. Der Vormischbereich von Gasturbinenbrennern ist nicht für hohe Temperaturen ausgelegt - ein Flammenrückschlag kann daher zu einer schweren Schädigung der Brennerhardware führen.

Im Projekt "Flash-GT" wurde der Flammenrückschlag von Wasserstoff-Methan-Luft-Flammen in der Wandgrenzschicht von verdrallten Strömungen durch Experiment und Modellierung untersucht. Für die experimentellen Arbeiten wurde der Hochdruckprüfstand am PSI mit einem optisch zugänglichen Drallbrenner ausgerüstet. Zur numerischen Untersuchung der Flashback-Ereignisse wird eine auf Large-Eddy-Simulation (LES) basierende CFD-Modellierung angewendet.

Die Rückschlaggrenzen wurden systematisch für einen weiten Bereich von bis zu 7,5 bar Brennkammerdruck und 300°C Vorwärmtemperatur untersucht. Der Einfluss von Druck, Verbrennungslufttemperatur, Wasserstoffgehalt, Vormischstrategie, Drall und Strömungsgeschwindigkeit auf die Flashback-Grenze wurde für gut kontrollierte Randbedingungen quantifiziert. Die erstellte Datenbank dient als Validierungsdatenbasis für die Flashback-Modellierung.

Hochgeschwindigkeits-Chemilumineszenz und 2D-laserinduzierte Fluoreszenz des OH-Radikals wurden zur Untersuchung des Flammenausbreitungsweges und der Flammenstruktur eingesetzt. Die Ergebnisse zeigen, dass es zwei verschiedene Flammenausbreitungspfade bei einem Flammenrückschlag in der Grenzschicht einer Drallflamme gibt, wobei die Drallzahl der wichtigste Parameter ist, der die beiden Varianten unterscheidet (bei niedrigem Drall breitet sich die Flamme entgegen der Drallrichtung aus, bei hohem Drall breitet sie sich mit der Drallrichtung aus).

Mit Particle Image Velocimetry (PIV)-Messungen wurde das Geschwindigkeitsfeld im Vormischbereich des Drallbrenners bestimmt. Die erhaltenen Geschwindigkeitsprofile dienen dabei auch als Eingangs- und Validierungsdaten für die Strömungsmodellierung.

Es wurden zudem chemisch-kinetische Berechnungen von eindimensionalen, gestreckten Flammen unter den Bedingungen des Flammenrückschlags durchgeführt. Die Ergebnisse zeigen, dass bei einem Druck von 2,5 bar und einer Vorwärmtemperatur von 200° die Flammen in einem breiten Bereich von Wasserstoffgehalt im Brenngas und Äquivalenzverhältnis zum Zeitpunkt des Flammenrückschlags eine gemeinsame kritische Dehnungsrate aufweisen. Diese Erkenntnis bietet einen wichtigen Hinweis, um darauf basierend Modelle zur verbesserten Vorhersage von Flammenrückschlaggrenzen zu entwickeln.

Die LES-Modellierung in dieser Arbeit wurde mit einem kompressiblen reaktiven Code mit Subfiltermodellen für Turbulenz und chemische Quellterme durchgeführt. Ein detaillierter Wasserstoffmechanismus mit neun chemischen Spezies und neunzehn Reaktionen wurde zur Modellierung der chemischen Reaktionen verwendet. Die Modellierung des vollständigen Flashback-Prozesses ist aufgrund der extrem langen Simulationszeiträume zwar rechnerisch nicht durchführbar, Flashback-Grenzen (d.h. der Beginn des Flammenrückschlags) können aber bestimmt werden. Die simulierten Flashback-Grenzen liegen dabei im Vergleich zu den experimentellen Messungen recht nahe beieinander. Außerdem werden die Trends der Flashback-Grenzen für verschiedene Betriebsparameter korrekt wiedergegeben. Eine detaillierte Analyse der Berechnungsergebnisse liefert darüber hinaus wertvolle zusätzliche Erkenntnisse über die Wechselwirkung zwischen der Flammenfront und dem

Strömungsfeld in Wandnähe während des Flammenrückschlags. Die Simulationen liefern eine Fülle von Daten, mit denen das Flammenverhalten in der Nähe der Flammenrückschlagsgrenze untersucht werden kann, um die Modelle für die Vorhersage von Flammenrückschlagsgrenzen zu verbessern. Die Simulationen bieten auch die Möglichkeit, den Flammenrückschlag anhand von Größen, die experimentell extrem schwer zu messen sind, besser zu verstehen.

Da keines der in der Literatur beschriebenen Modelle zur Flammenrückschlagsvorhersage in der Lage ist, die Flammenrückschlagsgrenzen der gegenwärtig untersuchten Konfiguration genau zu erfassen, wurde ein neuartiges Modell entwickelt und geprüft, das tatsächlich zu solchen Vorhersagen in der Lage ist. Ein solches Modell ist ein wichtiges Werkzeug für die Industrie und wird weiterentwickelt.

Bei der Untersuchung der experimentell gemessenen Rückschlaggrenzen des Drallbrenners am PSI zeigte sich, dass bei gegebener Strömungsgeschwindigkeit die Extinktionsdehnungsrate einer eindimensionalen gedehnten Flamme bei den gegebenen thermochemischen Bedingungen (d.h. Temperatur, Druck und Äquivalenzverhältnis) einen konstanten Wert aufweist, wenn ein Flammenrückschlag auftritt. Das auf dieser Erkenntnis beruhende, neu entwickelte Berechnungsmodell ist in der Lage, hochgenaue Vorhersagen für die Flammenrückschlagsgrenze sowohl für nicht verdrallte Strömungen (Literaturdaten) als auch für verdrallte Strömungen (diese Studie) zu treffen. Das Modell kann verwendet werden, um den Wert des kritischen Wandgeschwindigkeitsgradienten bei einem bestimmten Rückschlagereignis zu ermitteln. Es wird erwartet, dass dieser Wandgeschwindigkeitsgradient hauptsächlich von der Einlassgeschwindigkeit und -geometrie abhängt. Daher sollte der ermittelte Wert auch dann gültig bleiben, wenn sich Temperatur, Druck, Wasserstoffgehalt usw. ändern, solange die Eintrittsgeschwindigkeit und die Geometrie unverändert bleiben. Der Gültigkeitsbereich kann noch erweitert werden, indem man annimmt, dass sich bei konstanter Geometrie der Wandgeschwindigkeitsgradient linear mit der Einströmgeschwindigkeit ändert. Dann sollte eine einzige experimentelle Messung in Verbindung mit dem Modell in der Lage sein, die Rückschlaggrenzen eines bestimmten Brenners auch bei Änderung der thermochemischen und Strömungsbedingungen vorherzusagen. Wenn dies für einige verschiedene Brennergeometrien und Strömungsbedingungen bestätigt werden kann, könnte sich das Modell zu einem mächtigen Werkzeug für die Vorhersage von Rückschlaggrenzen entwickeln.

Um zu zeigen, dass das Modell auf verschiedene thermochemische Bedingungen anwendbar ist, wurden Rückschlaggrenzen vorhergesagt und mit experimentellen Messungen bei verschiedenen Druck-/Temperatur- und Brenngasmischungsbedingungen verglichen. Selbst über einen großen Bereich der Wandtemperatur reproduziert das Modell erfolgreich das Rückschlagverhalten des Systems. Da die Wandtemperatur eine wichtige Rolle bei der Kontrolle von Rückschlagereignissen spielt, ist diese Vorhersagefähigkeit des vorgestellten Modells von größter Bedeutung. Als wichtigste Empfehlung auf der Grundlage der erzielten Ergebnisse kann eine Kontrolle der Wandtemperatur (zumindest in bestimmten kritischen Zonen der Brenner/Mischer-Konfiguration) als sehr wirksam für die Unterdrückung des Grenzschicht-Flashback-Risikos bei Brenngasgemischen mit zunehmendem Wasserstoffanteil angesehen werden. Insofern scheint eine Neukonzeption von Gasturbinenbrennern (relativ leicht) machbar, die eine aktive Kühlung bestimmter kritischer Teile des Brenners vorsieht. Die lokale Kühlung in dieser Hinsicht kann sinnvollerweise mit (zwischengekühlter) Druckluft aus dem Gasturbinenkompressor erfolgen.

Wichtigste Ergebnisse (Take-Away Messages)

- Beim Flammenrückschlag in Wandgrenzschichten von Drallbrennern gibt es zwei Flammenausbreitungswege, wobei die Drallzahl der wichtigste Unterscheidungsparameter ist.
- Die experimentellen Messungen bei unterschiedlichen Druck-/Temperatur- und Brenngasgemischbedingungen haben (erneut) bestätigt, dass die Wandtemperatur eine äußerst wichtige Rolle bei der Kontrolle von Flammenrückschlag in Wandgrenzschichten spielt.

- Eine Kontrolle der Wandtemperatur (zumindest in bestimmten kritischen Zonen der Brenner-/Mischerkonfiguration) kann als sehr wirksam für die Unterdrückung des Rückschlagrisikos bei Brenngasgemischen mit zunehmenden Wasserstoffanteilen angesehen werden.
- Bei einer Anpassung von Gasturbinenbrennern (Neukonstruktion oder Nachrüstung) sollte eine aktive Kühlung (durch Luft oder Wasser) bestimmter kritischer Teile des Brenners in Betracht gezogen werden.
- Keines der in der Literatur beschriebenen Modelle zur Vorhersage des Flammenrückschlags ist derzeit in der Lage, die Grenzen des Flammenrückschlags bei der untersuchten generischen Drallbrennerkonfiguration genau zu erfassen.
- Ein in diesem Projekt entwickeltes neues Modell (auf der Grundlage eines Kriteriums für die kritische Dehnungsrate, die zu Flammenlöschen führt) ist in der Lage, hochpräzise Vorhersagen über die Rückschlaggrenze bei nicht verdrallten Strömungen (validiert mit Literaturdaten) sowie bei verdrallten Strömungen (validiert mit experimentellen Daten aus dieser Studie) zu treffen.
- Das neue Modell kann mit einer einzigen experimentellen Messung für eine bestimmte Brennergeometrie kalibriert werden und kann dann zur Vorhersage der Rückschlaggrenzen für eine Vielzahl von thermochemischen und Strömungsbedingungen verwendet werden.
- Das Modell kann für eine Vielzahl unterschiedlicher Brennergeometrien und Strömungsbedingungen verwendet werden und kann den Brennerauslegungsprozess in Richtung von Brennergeometrien lenken, die Rückschlagereignisse wirksam verhindern.

Summary

Gas turbines offer high reliability combined with an excellent load following capability, attributes which become ever more important in the future energy supply infrastructure. Furthermore, lean-premixed combustion in gas turbines achieves remarkably low emissions compared to burning liquid or solid fuels. However, the current generation of burners was mainly developed to operate on natural gas and is limited to narrow operational windows in terms of fuel/air ratio to prevent operability issues. These burners are challenged by the desire to run gas turbines on alternative, renewable fuels, which typically contain large amounts of hydrogen. A key technical issue when burning fuels containing large amounts of hydrogen is to prevent flame flashback into the premix section. The premix section of gas turbine combustors is not designed to handle high temperatures; hence, flashback can lead to a severe failure of the burner hardware.

In the project “Flash-GT” flame flashback of hydrogen-methane air flames in the boundary layer of swirling flows has been investigated through experiment and modelling. For the experimental work, the high-pressure test rig at PSI has been equipped with an optically accessible swirl burner. Large-eddy simulation based CFD is applied to investigate the flashback events numerically.

Flashback limits have been investigated systematically for a wide range of conditions up to 7.5bar and 300°C preheat temperature. The effect of pressure, preheat temperature, hydrogen content, premix strategy, swirl and bulk flow velocity on the flashback limit has been quantified for well-controlled boundary conditions. The compiled database serves as validation data for flashback modelling.

High-speed chemiluminescence and planar-laser induced fluorescence imaging of the OH radical have been applied to study the flame propagation pathway and flame structure. The results show that two distinct flame propagation pathways exist in swirl flame boundary layer flashback, with swirl number being the dominant parameter distinguishing between the two (at low swirl - flame propagates against the direction of swirl; at high swirl - flame propagates with the direction of swirl).

Particle image velocimetry measurements have provided the velocity field in the premix section of the swirl burner. The velocity profiles serve as an input and validation data for all modelling activities.

Chemical kinetics computations of one-dimensional, stretched flames at the conditions of flame flashback have been conducted. The results show that at a fixed pressure of 2.5bar and 200° preheat temperature, flames across a wide range of hydrogen content and equivalence ratio all share a common critical stretch rate at the instant of flashback. This finding offers a pathway for improved models to predict a flashback limit.

The LES (Large Eddy Simulation) modeling in this work was performed using a compressible reactive code with subfilter models for turbulence and chemical source terms closure. A detailed hydrogen mechanism with nine chemical species and nineteen reactions was used to model chemical reactions. Mimicking the full flashback process computationally is unfeasible because of the extremely long simulation timescales needed. The simulated flashback limits are reasonably close compared to the experimental measurements. In addition, flashback limit trends for various operating parameters are captured correctly. A detailed analysis of the computational results produces valuable additional insight into the relationship between the flame front and the flow conditions near the wall during flashback. The simulations provide an abundance of data with which the flame behavior near the flashback limit can be studied to help improve flashback limit models. The simulations provide an opportunity to better understand flashback through quantities difficult to measure experimentally.

As none of the flashback prediction models reported in literature is capable of accurately capturing the flashback limits of the presently studied configuration, a new type of model is developed and presented that is actually capable of such predictions. Such a model remains an important tool for industry and will be further developed in this direction.

Examining the experimentally measured flashback limits from the swirling burner at the Paul Scherrer Institute, it became apparent that – at a given bulk flow velocity - the extinction strain rate of a one-dimensional strained flame remains constant at the given thermochemical conditions (i.e., temperature, pressure, and equivalence ratio) when flashback occurs. The newly developed model is capable of highly accurate flashback limit predictions in non-swirling flows (literature data), as well as for swirling flows (this study). The model can be used to find the value of the critical wall velocity gradient at a given flashback event. This wall velocity gradient is expected to be a function mainly of the inlet velocity and geometry. Thus, the value extracted should remain valid even as temperature, pressure, hydrogen content, etc. change, so long as the inlet velocity and geometry remain unchanged. This can be extended even further by assuming that, for a constant geometry, the wall velocity gradient will change linearly with the inlet flow velocity. Then, a single experimental measurement combined with the model should be able to predict the flashback limits within a given combustor even with changes in the thermochemical and flow conditions. If this can be confirmed for a few different burner geometries and flow conditions, the model might evolve as a mighty tool for flashback limit predictions.

In order to show that the model is applicable to various thermochemical conditions, flashback limits are predicted and compared to experimental measurements at different pressure/temperature and fuel gas mixture conditions. Even across a large range in wall temperature, the model does successfully reproduce the flashback behavior of the system. As wall temperature plays an important role in controlling flashback events, this predictive capability of the presented model is of utmost importance. As a major recommendation based on the results achieved, a control of the wall temperature (at least in certain critical zones of the burner/mixer configuration) can be considered very effective for the suppression of the boundary layer flashback risk for fuel gas mixtures containing increasing amounts of hydrogen. To this extent a re-design of gas turbine burners seems (somewhat easily) feasible which should include active cooling of certain critical parts of the burner. The local cooling in this respect can be reasonably achieved with (inter-cooled) compressed air taken from the gas turbine compressor.

Main findings (take-away messages)

- Two distinct flame propagation pathways exist in boundary layer flashback of swirl burners, with swirl number being the dominant distinguishing parameter.
- It is (re-)confirmed by the experimental measurements at different pressure/temperature and fuel gas mixture conditions that the wall temperature plays an extremely important role in controlling boundary layer flashback events.
- A control of the wall temperature (at least in certain critical zones of the burner/mixer configuration) can be considered very effective for the suppression of the boundary layer flashback risk for fuel gas mixtures containing increasing amounts of hydrogen.
- A re-design of gas turbine burners (new design or retrofit) should consider active cooling (by air or water) of certain critical parts of the burner.
- None of the flashback prediction models reported in literature is currently capable of accurately capturing the flashback limits of the generic swirl burner configuration studied.
- A new model (based on a critical extinction strain rate criteria) developed in this project, is capable of highly accurate flashback limit predictions in non-swirling flows (validated with literature data), as well as for swirling flows (validated with experimental data from this study).
- The new model can be calibrated with a single experimental measurement for a given burner geometry, and can then be used to predict the flashback limits for a variety of thermochemical and flow conditions.
- The model can be used for a variety of different burner geometries and flow conditions, and can guide the burner design process in the direction of burner geometries which effectively prevent flashback events.

Résumé

Les turbines à gaz offrent une grande fiabilité associée à une excellente capacité de suivi de la charge, des attributs qui deviennent de plus en plus importants dans la future infrastructure d'approvisionnement en énergie. En outre, la combustion en mélange pauvre dans les turbines à gaz permet de réduire remarquablement les émissions par rapport à la combustion de combustibles liquides ou solides. Cependant, la génération actuelle de brûleurs a été principalement développée pour fonctionner au gaz naturel et est limitée à des fenêtres opérationnelles étroites en termes de ratio carburant/air pour éviter les problèmes d'opérabilité. Ces brûleurs sont mis au défi par le désir de faire fonctionner des turbines à gaz avec des combustibles alternatifs et renouvelables, qui contiennent généralement de grandes quantités d'hydrogène. Un problème technique clé lors de la combustion de combustibles contenant de grandes quantités d'hydrogène est d'empêcher le retour de flamme dans la section de prémélange. La section de prémélange des chambres de combustion des turbines à gaz n'est pas conçue pour supporter des températures élevées ; le retour de flamme peut donc entraîner une défaillance grave du matériel du brûleur.

Dans le cadre du projet "Flash-GT", le retour de flamme des flammes hydrogène-méthane-air dans la couche limite des écoulements tourbillonnaires a été étudié par l'expériments et la modélisation. Pour le travail expérimental, le banc d'essai haute pression du PSI a été équipé d'un brûleur à tourbillon optiquement accessible. La CFD basée sur la simulation des grands tourbillons est appliquée pour étudier numériquement les phénomènes de retour de flamme.

Les limites du retour de flamme ont été étudiées systématiquement pour une large gamme de conditions allant jusqu'à 7,5 bars et 300°C de température de préchauffage. L'effet de la pression, de la température de préchauffage, de la teneur en hydrogène, de la stratégie de prémélange, du

tourbillon et de la vitesse d'écoulement globale sur la limite de retour de flamme a été quantifié pour des conditions limites bien contrôlées. La base de données compilée sert de données de validation pour la modélisation du retour de flamme.

La chimiluminescence à haute vitesse et l'imagerie planaire du fluorescence induite par laser du radical OH ont été appliquées pour étudier le chemin de propagation de la flamme et sa structure. Les résultats montrent que deux voies distinctes de propagation de la flamme existent dans le retour de flamme de la couche limite d'une flamme tourbillonnante, le nombre de tourbillons étant le paramètre dominant qui distingue les deux (à faible tourbillon - la flamme se propage contre la direction du tourbillon ; à tourbillon élevé - la flamme se propage avec la direction du tourbillon).

Les mesures de vélocimétrie par image de particules ont fourni le champ de vitesse dans la section de prémélange du brûleur à tourbillon. Les profils de vitesse servent de données d'entrée et de validation pour toutes les activités de modélisation.

Des calculs de cinétique chimique de flammes unidimensionnelles étirées dans les conditions d'un retour de flamme ont été effectués. Les résultats montrent qu'à une pression fixe de 2,5 bars et une température de préchauffage de 200°, les flammes d'une large gamme de teneur en hydrogène et de rapport d'équivalence partagent toutes un taux d'étirement critique commun au moment du retour de flamme. Cette découverte ouvre la voie à des modèles améliorés pour prédire la limite du retour de flamme.

La modélisation LES (Large Eddy Simulation) de ce travail a été réalisée à l'aide d'un code réactif compressible avec des modèles de sous-filtres pour la fermeture des termes de turbulence et de source chimique. Un mécanisme détaillé d'hydrogène avec neuf espèces chimiques et dix-neuf réactions a été utilisé pour modéliser les réactions chimiques. Il est impossible d'imiter le processus de retour de flamme complet sur le plan informatique en raison des échelles de temps de simulation extrêmement longues nécessaires. Les limites du retour de flamme simulées sont raisonnablement proches des mesures expérimentales. De plus, les tendances des limites de retour de flamme pour divers paramètres de fonctionnement sont correctement capturées. Une analyse détaillée des résultats de calcul fournit des informations supplémentaires précieuses sur la relation entre le front de flamme et les conditions d'écoulement près de la paroi pendant le retour de flamme. Les simulations fournissent une abondance de données avec lesquelles le comportement de la flamme près de la limite du retour de flamme peut être étudié pour aider à améliorer les modèles de limite du retour de flamme. Les simulations fournissent une opportunité de mieux comprendre le retour de flamme à travers des quantités difficiles à mesurer expérimentalement.

Comme aucun des modèles de prédiction du retour de flamme rapportés dans la littérature n'est capable de capturer avec précision les limites du retour de flamme de la configuration actuellement étudiée, un nouveau type de modèle est développé et présenté qui est réellement capable de telles prédictions. Un tel modèle reste un outil important pour l'industrie et sera développé plus avant dans cette direction.

En examinant les limites de retour de flamme mesurées expérimentalement dans le brûleur à tourbillon de l'Institut Paul Scherrer, il est apparu que, pour une vitesse d'écoulement donnée, le taux de déformation d'extinction d'une flamme déformée unidimensionnelle reste constant dans des conditions thermochimiques données (c'est-à-dire la température, la pression et le rapport d'équivalence) lorsque le retour de flamme se produit. Le modèle nouvellement développé est capable de prédire avec une grande précision la limite du retour de flamme dans les écoulements non tourbillonnaires (données de la littérature), ainsi que pour les écoulements tourbillonnaires (cette étude). Le modèle peut être utilisé pour trouver la valeur du gradient de vitesse critique de la paroi lors d'un retour de flamme donné. Ce gradient de vitesse de paroi est censé être une fonction principalement de la vitesse et de la géométrie d'entrée. Ainsi, la valeur extraite devrait rester valide même si la température, la pression, la teneur en hydrogène, etc. changent, tant que la vitesse et la géométrie d'entrée restent inchangées. On peut aller encore plus loin en supposant que, pour une géométrie constante, le gradient de vitesse de la paroi évolue linéairement avec la vitesse d'entrée. Alors, une seule mesure expérimentale combinée au modèle devrait pouvoir prédire les limites du retour de flamme dans une chambre de combustion donnée, même avec des changements dans les conditions thermochimiques et d'écoulement. Si cela peut être confirmé pour quelques géométries de brûleurs et conditions d'écoulement différentes, le modèle pourrait devenir un outil important pour la prédiction des limites du retour de flamme.

Afin de montrer que le modèle est applicable à diverses conditions thermochimiques, les limites de retour de flamme sont prédites et comparées aux mesures expérimentales à différentes conditions de pression/température et de mélange de gaz combustible. Même dans une large gamme de température de paroi, le modèle reproduit avec succès le comportement de retour de flamme du système. Comme la température de la paroi joue un rôle important dans le contrôle des événements de retour de flamme, cette capacité de prédiction du modèle présenté est de la plus haute importance. Comme recommandation majeure basée sur les résultats obtenus, un contrôle de la température de la paroi (au moins dans certaines zones critiques de la configuration brûleur/mélangeur) peut être considéré comme très efficace pour la suppression du risque de retour de flamme de la couche limite pour les mélanges de gaz combustible contenant des quantités croissantes d'hydrogène. Dans cette mesure, une nouvelle conception des brûleurs de turbine à gaz semble (assez facilement) réalisable, qui devrait inclure un refroidissement actif de certaines parties critiques du brûleur. Le refroidissement local à cet égard peut être raisonnablement réalisé avec de l'air comprimé (inter-refroidi) provenant du compresseur de la turbine à gaz.

Principaux résultats (Take-Away Messages)

- Lors du retour de flamme dans les couches limites des parois des brûleurs à tourbillon, il existe deux voies de propagation de la flamme, le nombre de tourbillons étant le paramètre de distinction le plus important.
- Les mesures expérimentales effectuées dans différentes conditions de pression/température et de mélange de gaz combustible ont (à nouveau) confirmé que la température de paroi joue un rôle extrêmement important dans le contrôle du retour de flamme dans les couches limites de la paroi.
- Le contrôle de la température de paroi (au moins dans certaines zones critiques de la configuration du brûleur/mélangeur) peut être considéré comme très efficace pour supprimer le risque de retour de flamme dans les mélanges de gaz combustibles contenant des quantités croissantes d'hydrogène.
- Lors de l'adaptation des brûleurs de turbine à gaz (nouvelle conception ou mise à niveau), il convient d'envisager un refroidissement actif (par air ou par eau) de certaines parties critiques du brûleur.
- Aucun des modèles de prédiction du retour de flamme décrits dans la littérature n'est actuellement en mesure d'appréhender avec précision les limites du retour de flamme dans la configuration générique du brûleur à tourbillon étudiée.
- Un nouveau modèle développé dans le cadre de ce projet (basé sur un critère de taux de déformation critique conduisant à l'extinction de la flamme) est capable de prédire avec une grande précision la limite de retour de flamme pour des écoulements non torsadés (validés avec des données de la littérature) ainsi que pour des écoulements torsadés (validés avec des données expérimentales issues de cette étude).
- Le nouveau modèle peut être calibré à l'aide d'une seule mesure expérimentale pour une géométrie de brûleur donnée et peut ensuite être utilisé pour prédire les limites de rebond pour une variété de conditions thermochimiques et d'écoulement.
- Le modèle peut être utilisé pour une grande variété de géométries de brûleur et de conditions d'écoulement et peut orienter le processus de conception du brûleur vers des géométries de brûleur qui empêchent efficacement les événements de retour de flamme.

Contents

Abbreviations

BLF: Boundary Layer Flashback

CERFACS: Centre Européen de Recherche et de Formation Avancée en Calcul Scientifique

CFD: Computational Fluid Dynamics

CHP: Combined heat and power

CL: Chemiluminescence

LES: Large-eddy simulation

LIF: Laser Induced Fluorescence

MGT: Micro gas turbine

OH-PLIF: Laser Induced Fluorescence of the OH radical

PIV: Particle Imaging Velocimetry

PLIF: Planer-laser induced fluorescence

TIT: Turbine Inlet Temperature

TRL: Technical readiness level

UV: Ultraviolet

1 Introduction

1.1 Background information and current situation

1.1.1 The role of gas turbines for a future, sustainable energy supply

Gas turbines offer high reliability combined with an excellent load following capability, attributes which become ever more important in the future energy supply infrastructure. Furthermore, lean-premixed combustion in gas turbines achieves remarkably low emissions compared to burning liquid or solid fuels. However, the current generation of burners was mainly developed to operate on natural gas and is limited to narrow operational windows in terms of fuel/air ratio to prevent operability issues. These burners are challenged by the desire to run gas turbines on alternative, renewable fuels, which typically contain large amounts of hydrogen (ETN Global, 2020). High hydrogen content fuels may result from a power-to-gas storage approach, from pre-combustion CO_2 capturing methods employing fossil-fuel decarburization, or by using biogases. A key technical issue when burning fuels containing large amounts of hydrogen is to prevent flame flashback into the premix section. The premix section of gas turbine combustors is not designed to handle high temperatures; hence, flashback can lead to a severe failure of the burner hardware. An example of a commercial gas turbine combustor and damage due to flashback is shown in Figure 1 .

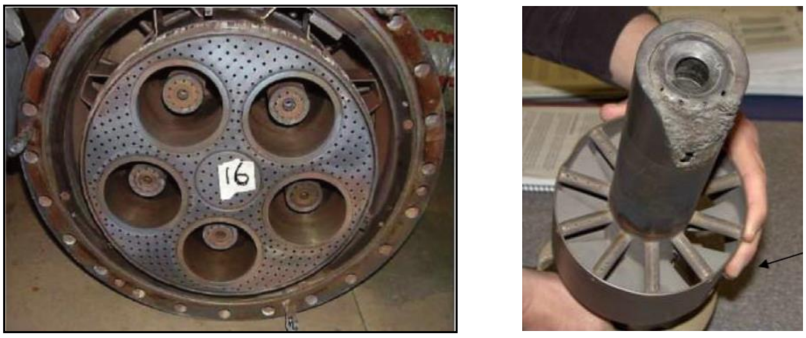

(a) (b)

Figure 1: (a) Combustion chamber with five lean-premix burners. (b) Damage to the central bluff body due to flashback (Meher-Homji et al., 2010).

Preventing flashback has not been the major design challenge for burners operating on natural gas owing to the low reactivity of methane. However, designing flashback resistant burners for more reactive fuels is significantly more challenging, resulting in a clear need for a better fundamental understanding of the underlying mechanisms with improved models to predict flashback limits, i.e. operational conditions (pressure, temperature, stoichiometry, flow velocity) for which flashback events occur (or not occur).

1.1.2 Importance for Next Generation Micro Gas Turbines

Decentralized power generation with combined heat and power (CHP) systems delivers a number of benefits, which include avoiding wasted heat and reducing transmission and distribution losses. Distributed, flexible CHP systems can further stabilize the electrical grid and thus reduce investment in the energy system infrastructure. Micro gas turbines (MGTs) are particularly suited as CHP units for a number of reasons including high reliability, low-maintenance costs, high exhaust gas temperatures and ultra-low emissions. In addition, the CO_2 footprint can be reduced (or eliminated) if part (or even all) of the natural gas fuel stream is replaced with renewable or off-product hydrogen.

However, burners for MGTs that run on high hydrogen content fuels or even pure hydrogen while at the same time meeting stringent emissions regulations without expensive post-combustion measures are not available (TRL 3). One of the main, unsolved challenges for MGTs to be operated on hydrogen rich fuels is to prevent flame flashback – similar to their large counter parts. For MGTs, even though they operate at lower pressure levels compared to their large counter parts, developing and designing flashback resistant burners for H_2-richt fuels is equally challenging. The reason is that MGTs are typically equipped with a recuperator that transfers heat from the exhaust gases to the compressed air upstream of the combustor in order to increase the electrical efficiency. Operation with high preheat temperatures significantly increases the risk for flashback owing to the higher flame speeds and shorter autoignition delay times.

1.2 Purpose of the project

The purpose of this project is to support the development and design of fuel-flexible, lean-premixed gas turbines burners that are suitable for hydrogen-rich fuel mixtures. On the one hand, the project aims to advance the fundamental understanding of the physics of flame flashback. On the other hand, the purpose of the project is to provide practical engineering guidelines, which directly support the engineering process of developing and designing flashback resistant burners for fuel mixtures containing significant, varying amounts of H_2. For this reason, the focus is on investigating flashback that occurs in the boundary layer of swirling flows as this is directly relevant for typical gas turbine burners. Furthermore, the project directly targets operating conditions in terms of pressure and preheat temperature that are sufficiently close to and thus relevant for stationary gas turbines and MGTs.

Finally, the project aims at providing answers how well a state-of-the-art Large Eddy Simulation (LES) based CFD approach is capable of capturing and predicting boundary layer flashbacks and thus serve as a reliable tool in the engineering process of designing such burners.

1.3 Objectives

The first objective is to design, built and install a generic, optically accessible swirl burner in a high-pressure test rig to investigate flame flashback experimentally at conditions relevant for gas turbines. The objective of this experimental approach is two-fold. First, a large database of measured flashback limits is compiled. This database provides direct information for engineers how strongly a certain change in one particular operating condition affects the flashback margin. Furthermore, the large set of measured flashback limits serves as validation data for improved analytical models to predict a flashback limit. It will further be used to assess the accuracy of LES based CFD simulations of flashback events.

The second objective is to apply high-speed imaging and advanced laser-based measurement techniques to improve the understanding of the fundamental physics of flashback. The focus will be on studying the transient, upstream flame propagation inside the premix section during flashback events. The dominant mechanisms facilitating flashback in the boundary layer of swirling flows are not yet fully understood and will be addressed.

The third objective is to apply a particular LES based modelling approach for reacting flows, which has shown great strength in simulating combustion phenomena in practical geometries, to swirl flame boundary layer flashback. The goal is to understand whether this particular modelling approach captures the relevant physics of boundary layer flashback sufficiently accurate to serve as an engineering tool for developing flashback resistant burners. LES simulations will also aid in improving the fundamental understanding of boundary layer flashback.

In conclusion, the objective of the project is to provide more precise recommendations for designing flashback resistant burners for H_2-rich fuel mixtures. These recommendations will be derived both from practical measurements in the high-pressure test rig as well as from new insights into the detailed physics of boundary layer flashback. The objectives are summarized in Figure 2.

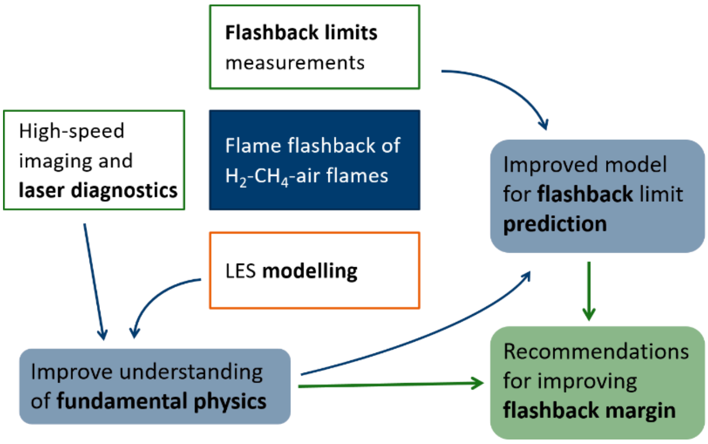

Figure 2: Project objectives of the joint experimental-computational approach.

2 Description of experimental facility

A new, optically accessible swirl burner was designed and installed in the high-pressure test rig at PSI for the experimental investigations of the project as shown in Figure 3. Optical access to the entire premix section and combustion chamber is provided through three large windows in the test rig. Swirl is generated with eight-bladed axial swirler elements. The swirler elements were additively manufactured out of stainless steel to generate various swirl numbers, i.e. with blade angles with respect to the burner axis of 0°, 40°, 50°, 55° and 65°. One example is shown in Figure 4. The blade leading edges had an elliptical shape with radius 1.25~mm (minor axis, i.e. blade thickness) and 2.25~mm (major axis), respectively. The trailing edges were sharp.

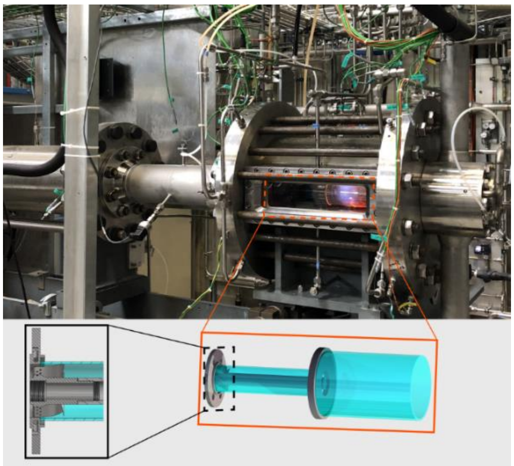

Figure 3: High-pressure test rig with new swirl burner in operation.

Figure 4: Axial swirler with 50° trailing edge angle.

Fuel can be injected through ports in the swirler vanes as is typically done in real gas turbines (technical premixing), or – far - upstream of the swirler (perfectly premixed conditions), which eliminates equivalence ratio stratifications for fundamental studies focusing on aspects other than the effect of fuel-air mixing. In the latter case, fuel is injected into the preheated air 430 mm upstream of the swirler through a cross-shaped tubing arrangement with 25 ports distributed across various radial and circumferential locations. In addition, a static mixture (STAMIXCO 18-315) is installed downstream of the fuel injection location to ensure fully premixed conditions already at the burner mixing tube inlet.

A cross section of the burner is shown in Figure 5. The diameter of the swirler hub and the attached cylindrical bluff body (center body) is 18 mm. The center body, which is made of AISI 316L stainless steel, ends flush with the mixing tube exit. It is hollow (wall thickness: 3 mm) to allow for internal cooling.

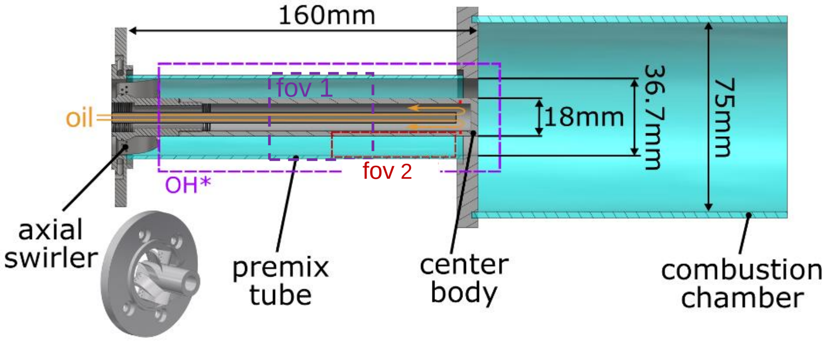

Figure 5: Swirl burner cross section with main dimensions. The oil circuit for center body heating/cooling is indicated in orange. Field-of-view (fov) areas for camera observation are indicated in purple.

The fused silica tube (Suprasil 310) of the premix section has an inner diameter of 36.7 mm. It is sealed against the swirler plate and burner head with graphite rings. Spring-loaded bolts fix the burner head against the swirler plate and thus allow for thermal expansion of the premix tube. The combustion chamber consists of a fused silica tube with an inner diameter of 75 mm and a length of about 150 mm.

The wall temperature of the center body is actively controlled by an internal oil circuit as indicated in Figure 5. High-temperature oil (maximum 300°C) is electrically heated or cooled with an oil-water heat exchanger to maintain a desired temperature. The oil enters the center body through an inner, concentric tube and exits through the annulus between inner tube and center body wall. The center body is equipped with two thermocouples located near its tip (red squares in Figure 5).

Thermal mass flow controllers (Bronkhorst) are used to control the methane and hydrogen flow rates. The main air was controlled with the combination of a thermal flow meter (Bronkhorst) and a needle-valve. All flow meters were re-calibrated prior to the measurement campaigns. The burner was ignited with a spark-ignited hydrogen torch located in the burner head at the entrance of the combustion chamber.

3 Experimental procedures and numerical methodologies

3.1 Flashback limit measurements

Flashback limits were measured for a range of pressures, preheat temperatures, bulk flow velocities in the premix section, hydrogen volume fractions in the fuel mixture and swirl numbers as summarized in Table 1. Flashbacks were triggered by first establishing a lean flame at a desired nominal operating point (p, T_{pre}, u_{bulk}, X_{H2}) followed by increasing the equivalence ratio ϕ at a constant, slow rate of Δλ=0.1

per minute, where $\phi = 1/\lambda$. The LabView based control system increased ϕ by simultaneously increasing fuel mass flow rates and decreasing the air flow rate while keeping p, T_{pre}, u_{bulk} and X_{H2} constant.

Table 1: Range of operating conditions covered for flashback limit measurements

pressure p	1 – 7.5 bar
preheat temperature T_{pre}	100 – 300 °C
inlet velocities u_{bulk}	15 – 40 m/s
volume fraction of H_2 in H_2-CH_4 mixture X_{H2}	(30)/50 – 100%
fuel injection strategy	perfect and technical premixing
swirl vane angles	0°, 40°, 50°, 55°, 65°

The center body wall temperature, controlled by an oil heating/cooling system as described in Section 2, was matched to the preheat temperature for all experimental studies, especially for the flashback limit measurement studies, except where noted otherwise. This has the important consequence that the relationship between a flashback limit and a control parameter (such as the chamber pressure) presented in this work is uncoupled from an otherwise simultaneously occurring change in metal wall temperature. Generally, changing any parameter such as p, T_{pre}, u_{bulk} or X_{H2} will shift the flame closer to or away from the wall, thus altering the heat load on the center body, changing the wall temperature and affecting the flashback limit.

The preheat temperature reported in this work corresponds to the temperature at the mixing tube exit. It is derived from the continuously measured gas temperature immediately upstream of the swirler combined with a correction factor accounting for the heat loss along the premix tube. This correction factor is determined based on a set of non-reacting, preheated flow measurements with an additional thermocouple installed at the entrance to the combustion chamber. For high preheat temperatures, i.e. large temperature differences driving the heat loss across the premix tube, this correction factor reaches up to 5 % of T_{pre}.

3.2 High-speed imaging and laser-diagnostics

In order to characterize the flame propagation pathway and the flame shape at the onset and during flashback events, high-speed chemiluminescence (CL) imaging and planar laser-induced fluorescence (PLIF) imaging of the OH-radical are applied.

The OH* luminescence was imaged with a LaVision HS-IRO intensifier lens-coupled to a LaVision HSS6 high-speed camera. The camera system was equipped with a Cerco 100 mm f/2.8 UV lens and a bandpass interference filter centered at 310 nm. Images were typically recorded at a repetition rate of 5 kHz.

PLIF measurements were conducted with the same detection system. The OH radical was excited with the frequency-doubled output of a dye laser (Radiant Dyes NarrowScan HighRep), which was pumped with the second harmonic (532 nm) output of a diode-pumped Nd:YAG laser (Edgewave IS400). The laser output was tuned to the $Q_2(8)$ transition of the A-X (ν'=1, ν''=0) band near 284 nm. UV pulse energies of about 1 mJ were achieved at 5 kHz repetition-rate. The laser beam was expanded into a collimated sheet and entered the high-pressure rig through a downstream window to illuminate one side of the annulus as shown in Figure 6.

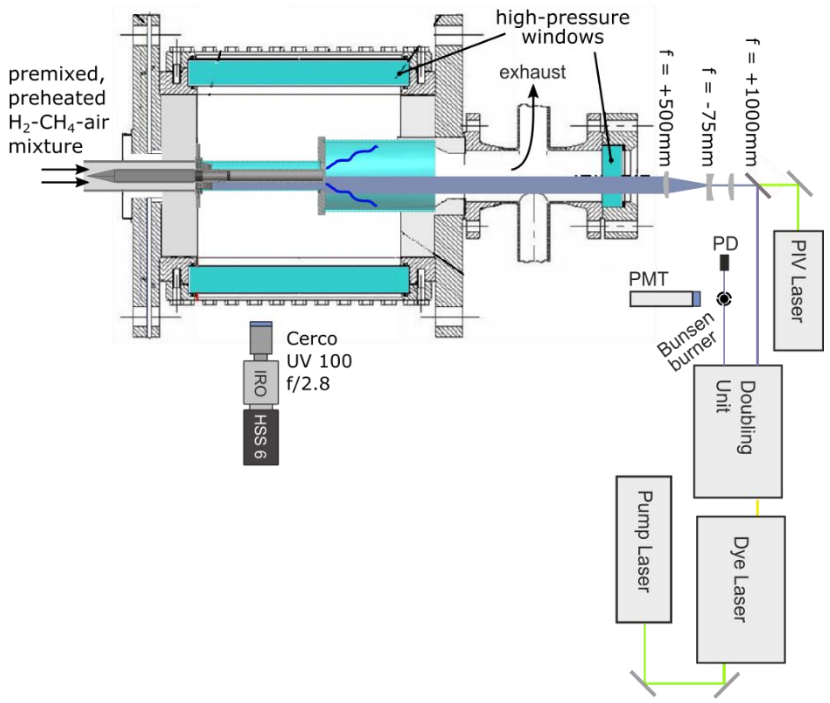

Figure 6: Setup for high-speed imaging and laser diagnostics.

Planar, two-component particle image velocimetry (PIV) was applied to characterize the non-reacting velocity field in the premix section. Alumina particles were seeded into the flow upstream of the static fuel-air mixer. The seeding air was controlled with an additional mass flow controller. To maximize the measurement time in between window cleaning, a high-speed PIV system was employed. The particles were illuminated with a Nd:YLF laser (Quantronix Darwin Duo) at 4~kHz, formed into a sheet with the same optics that were used for the PLIF. The sheet was carefully adjusted to graze along the center body wall, which minimized reflections, thus allowing velocity field measurements close to the center body. The particles were imaged with a LaVision HSS6 camera equipped with a 200 mm Nikon Micro-Nikkor lens (f/5.6) and a pixel resolution of 0.021 mm.

The PIV processing was done with the LaVision software DaVis 8.4. A standard multi-pass cross-correlation approach with decreasing interrogation window size and window deformation was employed. The final interrogation window size was 16 x 16 pix^2, with 50% overlap. The final cross-correlation was performed over a circular interrogation window with Gaussian weighting. The few spurious vectors were removed with a median filter and the resulting missing vectors were interpolated. The uncertainty was estimated based on the correlation statistics approach (Wieneke, 2015), which yielded about 3 to 5% in the core flow and up to 15% in the boundary layer close to the wall. The uncertainty in the wall-normal spatial location of each measured velocity vector due to challenges in identifying the wall location based on a light sheet reflection in the particle images was estimated to be about 3 pixels (≈0.06 mm).

3.3 Chemical kinetics computations

Equilibrium computations, auto-ignition delay time computations and one-dimensional, adiabatic flame simulations have been conducted using Cantera to support various aspects throughout this project. All adiabatic flame temperatures, auto-ignition delay times, unstretched and stretched laminar flame speeds as well as flame thicknesses reported in this work were computed using the AramcoMech 1.3

chemical mechanism, which has shown good performance for lean CH_4-H_2-air flames (Donohoe et al., 2014; Ji et al., 2017; Metcalfe et al., 2013).

3.4 LES Modelling

Swirl flame boundary layer flashback is modelled in this project by means of reactive Large-Eddy Simulations (LES). In LES, the large structures of the turbulent flow field are computed explicitly (i.e., resolved in space and time) whereas the effects of the smallest eddies are filtered out and need to be modelled. The filtered conservation equations to be solved may be written as [37]:

Mass: $\frac{\partial \bar{\rho}}{\partial t} + \frac{\partial(\bar{\rho}\tilde{u}_i)}{\partial x_i} = 0$

Momentum: $\frac{\partial(\bar{\rho}\tilde{u}_i)}{\partial t} + \frac{\partial(\bar{\rho}\tilde{u}_i\tilde{u}_j)}{\partial x_i} + \frac{\partial \bar{p}}{\partial x_j} = \frac{\partial}{\partial x_i}\left[\overline{\tau_{ij}} - \bar{\rho}\left(\widetilde{u_i u_j} - \tilde{u}_i\tilde{u}_j\right)\right]$

Chemical species: $\frac{\partial(\bar{\rho}\tilde{Y}_k)}{\partial t} + \frac{\partial(\bar{\rho}\tilde{u}_i\tilde{Y}_k)}{\partial x_i} = \frac{\partial}{\partial x_i}\left[\overline{V_{k,i}Y_k} - \bar{\rho}\left(\widetilde{u_i Y_k} - \tilde{u}_i\tilde{Y}_k\right)\right] + \overline{\dot{\omega}_k},\ k = 1 \ldots N$

Enthalpy: $\frac{\partial(\bar{\rho}\tilde{h}_s)}{\partial t} + \frac{\partial(\bar{\rho}\tilde{u}_i\tilde{h}_s)}{\partial x_i} = \frac{\overline{Dp}}{Dt} + \frac{\partial}{\partial x_i}\left[\overline{\lambda\frac{\partial T}{\partial x_i}} - \bar{\rho}\left(\widetilde{u_i h_s} - \tilde{u}_i\tilde{h}_s\right)\right] + \overline{\tau_{ij}\frac{\partial u_i}{\partial x_j}} - \frac{\partial}{\partial x_i}\left[\overline{\rho\sum_{k=1}^{N} V_{k,i}Y_k h_{s,k}}\right] + \overline{\dot{\omega}_T}$

To close the set of equations, so-called sub-grid scale models need to be utilized for the unresolved Reynolds stresses $\left(\widetilde{u_i u_j} - \tilde{u}_i\tilde{u}_j\right)$, species fluxes $\left(\widetilde{u_i Y_k} - \tilde{u}_i\tilde{Y}_k\right)$, enthalpy fluxes $\left(\widetilde{u_i h_s} - \tilde{u}_i\tilde{h}_s\right)$, filtered laminar diffusion fluxes $\overline{V_{k,i}Y_k}$ and $\overline{\lambda\frac{\partial T}{\partial x_i}}$ and filtered chemical reaction rate $\overline{\dot{\omega}_k}$.

LES simulations are performed using the AVBP solver developed at CERFACS, France. This solver is designed to handle practical geometries and so can simulate the full experimental configuration (i.e., mixing section, swirler vanes, burner) with ease. In addition, the solver offers several sub-grid scale models and combustion models, including the Smagorinsky model for closure of unresolved turbulence terms and the thickened flame model for closure of unresolved reaction terms.

AVBP is a compressible LES solver, which distinguishes it from many other LES solvers that are based on a low-Mach number (incompressibility) assumption. In a compressible LES, pressure disturbances propagated at a finite speed (speed of sound) and acoustics, e.g. thermo-acoustic instabilities, can be investigated.

Utilizing a compressible LES solver is potentially crucial for boundary layer flashback simulations as well, since a recent study (Endres & Sattelmayer, 2019) showed that a low-Mach number based approach underestimates the blockage effect due to gas dilatation imposed by a flame on the approach flow. This blockage effect is generally negligible for the flow-flame interaction of flames propagating in free space (which is why low-Mach number solvers have been very successful in the combustion community as well). However, for flames propagating along a wall (e.g. during boundary layer flashback) where the flame interacts with low-momentum fluid, gas dilatation effects become important and a compressible solver is needed to quantitatively capture the resulting local blockage effect correctly.

4 Flashback visualization

4.1 High-speed imaging and laser-based measurements

4.1.1 The two distinct flame propagation pathways in swirl flame boundary layer flashbacks

Four chemiluminescence (CL) images out of a full movie sequence recorded at p = 2.5 bar, X_{H2} = 70%, $T_{pre,}$ = 200°C, Re = 30,000 with the 50° trailing edge angle swirler are shown in Figure 7a (false-color applied to grayscale images; corresponding field-of-view fov1 shown in Figure 5). The swirl flow direction is indicated by red arrows. The horizontal gray lines outline the center body. We find that the flashback is led by small-scale flame bulges facing the approach flow head-on as indicated by the yellow arrows, i.e. the flame propagates against the bulk flow swirl direction (red arrows). The same such dominant flame propagation pathway was observed for all operating conditions with swirl angles of 50° and below.

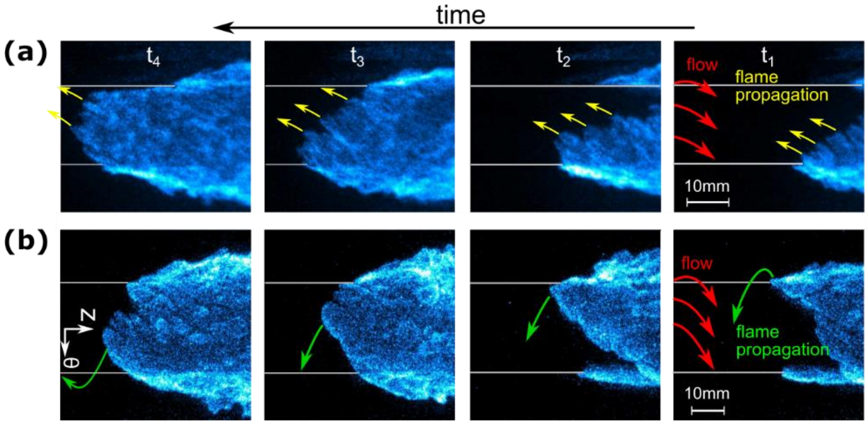

Figure 7: Two distinct flame propagation pathways: (a) 50° Swirler (b) 65° Swirler

In contrast, for swirler vanes angles above 55°, the flame was found to swirl in the direction of the bulk flow as shown in Figure 7b (indicated by the green arrow)}. Small-scale bulges did not achieve a sustained flame propagation against the bulk flow swirl direction. The relevant flow-flame interaction was entirely different and occurred on the leeward side of a larger flame front in agreement with previous studies on high-swirl flame flashbacks (Ebi et al., 2018; Ebi & Clemens, 2016).

The CL image sequences show that for low-swirl flame flashbacks the alignment between the flame propagation direction and the approach flow agrees with the alignment in a non-swirling BLF, i.e. head-on. In addition, the characteristic appearance of the leading flame front with its intermittent formation of small-scale flame bulges agrees well with previous studies in non-swirling flows (Eichler & Sattelmayer, 2012).

Finally, the recorded PLIF images for low swirl reveal a wedge-shaped, rather sharp flame leading edge in an axial-radial plane, which is the same for straight channel flashbacks as opposed to high swirl flame flashbacks, where a much more pronounced convex shape forms (Ebi et al., 2018). Hence, flashback events investigated in the current work may conceptually be viewed as non-swirling BLFs in a channel wound around the center body like a helical coil with the flow-flame interaction being driven by the same mechanisms as in a non-swirling BLF(Eichler & Sattelmayer, 2012; Gruber et al., 2012).

This is an important finding because models developed for non-swirling BLF should then also be applicable for flashback events up to a swirl number of about 0.7 given that the changes in the near-wall mean and r.m.s-velocity profiles due to swirl are correctly accounted for. These changes have to be incorporated in the model since swirl thickens the boundary layer along the inner (center body) wall compared to a non-swirling flow, which increases the flashback propensity (Ebi & Clemens, 2016). On the other hand, since the flame bulges align themselves in the low-momentum streaks of the turbulent boundary layer (Eichler & Sattelmayer, 2012; Gruber et al., 2012), they have to resist the momentum and strain associated with a boundary layer profile in the streamwise direction as opposed to merely the respective component in the axial direction. For a fixed mass flow (i.e., fixed u_{bulk}), the axial velocity on average remains constant, but the streamwise velocity opposing the flame propagation increases with an increase in swirl. This may at least partially counteract the previously described harmful thickening of the boundary layer when swirl is increased.

Finally, it is important to note that the flame already creeps upstream into the premix section along the center body wall by a distance on the order of 20 mm prior to a complete flashback, which is common for BLF in swirl burners with a central bluff body. In the literature, such flashbacks are referred to as confined flashbacks, meaning the flame is already confined inside the premix section prior to a complete flashback (Kalantari & McDonell, 2017). Different models have been developed for unconfined and confined flashback configurations to account for strong differences in the flashback propensity (Hoferichter et al., 2016, 2017).

4.1.2 Results of high-speed OH-PLIF imaging

A sample OH-PLIF image inside the premix section of a flashback event at 2.5 bar and with the 50° swirler is shown in Figure 8. The OH-PLIF images clearly show that the flame propagates along the center body wall. It has a rather sharp, convex (towards the reactants side) leading edge which resides close to the center body metal (< 1 mm). The bottom image in Figure 8 shows a mean flame shape. It is obtained by averaging single snapshots conditioned on the position of the leading edge of the flame. The overall flame shape resembles a sharp wedge.

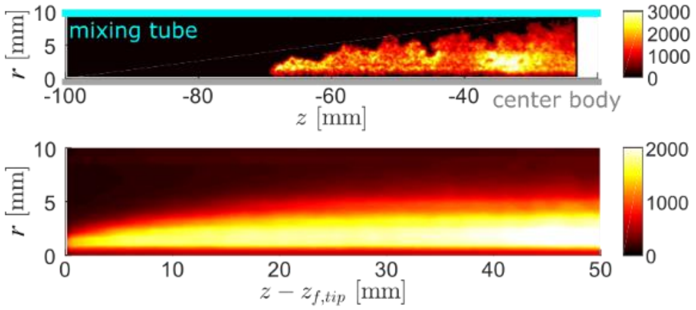

Figure 8: Single shot (top) and averaged (bottom) OH-PLIF image of flame inside premix section during a flashback event (field-of-view fov2 in Figure 5).

A sample OH-PLIF image sequence showing selected images inside the premix section from a flashback event at 7.5 bar is shown in Figure 9. The flame already creeps into the mixing section at conditions which are still too lean for a complete flashback all the way up to the swirler (see picture at time step TS94 in Figure 9). Once the equivalence ratio is reached where a full flashback occurs, the flame successively works its way upstream.

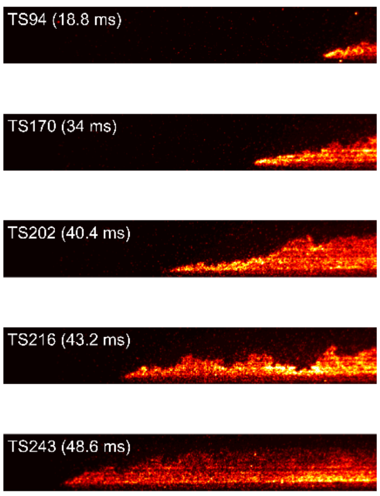

Figure 9: Selected time steps (TS) of a OH-PLIF image sequence showing flashback at 7.5bar, 300°C preheat temperature and 20m/s bulk flow velocity (field-of-view fov2 in Figure 5); flow direction: left - right

As the pressure is increased, the scale of the wrinkling of the flame surface decreases as expected (Figure 10). In addition, the radial flame spread decreases as the pressure is raised, which is in agreement with a recent LES study (Endres & Sattelmayer, 2019).

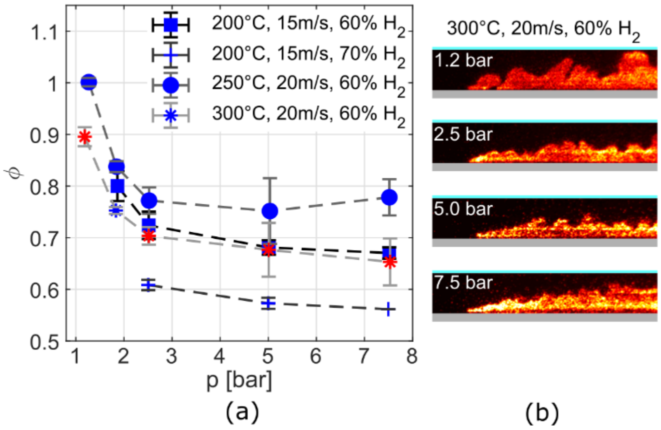

Figure 10: Effect of pressure on flame wrinkling and radial flame spread.

Beyond the general flame propagation pathway and flame shape, the high-speed OH-PLIF imaging only provides limited additional information beyond the line-of-sight OH* chemiluminescence imaging. The main reason is the three-dimensional flame propagation pathway in such flashbacks in the boundary layer of swirling flows.

5 Effects of pre-mixing quality on flashback limits

Non-perfect mixing between fuel and air leads to local variations in the equivalence ratio (equivalence ratio stratification). In lean-premix gas turbine burners, the goal typically is to achieve perfect mixing in the mixing section such that equivalence ratio stratifications at the entrance to the combustion chamber are negligible. However, some remaining unmixedness typically exists. The goal of this set of measurements was to investigate the effect of such unmixedness on flashback limits.

For this purpose, the fuel was injected through ports in the swirler vanes, which is a common strategy in real gas turbines (technical premixing). The resulting flashback limits are shown in red in Figure 11 for p=2.5bar, T_{pre}=200°C, u_{bulk}=20m/s and various hydrogen mole fractions. The flashback limits are compared to those obtained in the last funding period (blue symbols), where fuel and air were already perfectly premixed far upstream of the swirler. The results show that above 65% H_2, flashback occurs already at much leaner conditions for technical premixing conditions, i.e. the burner is more prone to experiencing flashbacks at otherwise equal operating conditions. The difference remains significant all the way up to pure hydrogen. On the other hand, at 60% H_2, flashback did not occur up to ϕ=0.8 (at this point the max. allowable heat load on the burner was reached). This suggests that at this operating condition and for H_2 contents below 60%, the same degree of unmixedness does not have a noticeable effect of the flashback limit.

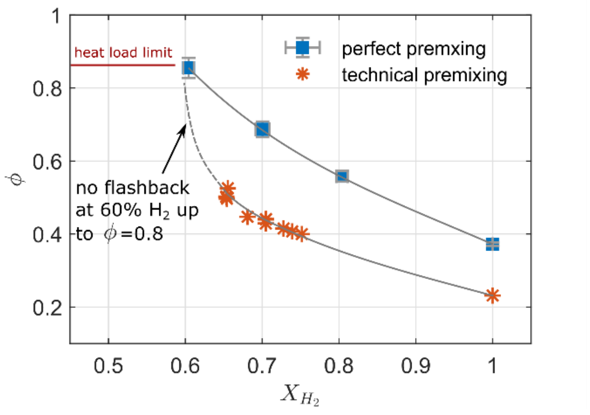

Figure 11: Comparison of flashback limits between perfect and technical premixing at p=2.5bar, T_{pre}=200°C, u_{bulk}=20m/s.

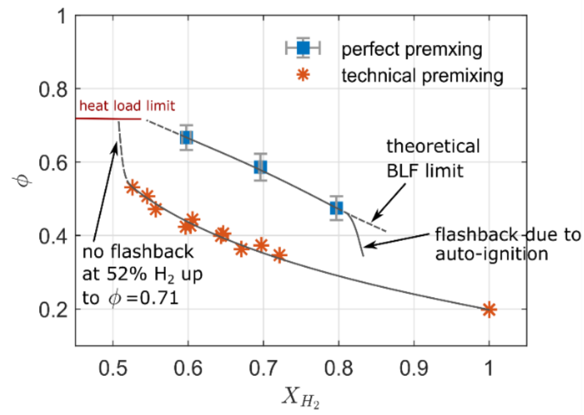

Figure 12: Comparison of flashback limits between perfect and technical premixing at p=5bar, T_{pre}=300°C, u_{bulk}=20m/s.

The same behaviour was observed at p=5bar, T_{pre}=300°C, u_{bulk}=20m/s (Figure 12). Here, the difference in the equivalence ratio at which flashback occurred differed significantly at about 55% H_2 and above. At this pressure and preheat temperature and for perfect premixing conditions, flashback at H_2 contents above 80% occurred due to auto-ignition instead of upstream flame propagation in the boundary layer. Therefore, a direct comparison up to 100% H2 was not possibly. However, the trendlines suggest the same behavior as for the lower pressure and preheat conditions.

The difference between the measured flashback limits for prefect premix vs. technical premix conditions is significant. The results emphasize that a well-designed premix section to reduce equivalence ratio stratifications is of high importance not only for minimizing NOx emissions but also for preventing flame flashback for H_2-CH_4-air flames with H_2 contents above about 50% (depends on exact operating condition).

This finding holds for the entire investigated range in pressure as shown in Figure 13. Here the flashback limits for a fuel mixture with 60% H_2 and for a pure H_2-air flame are shown. Both data sets show the same strong increase in flashback propensity as the pressure is raised from atmospheric conditions to about 3 bar as was previously observed for perfect premix conditions (blue symbols).

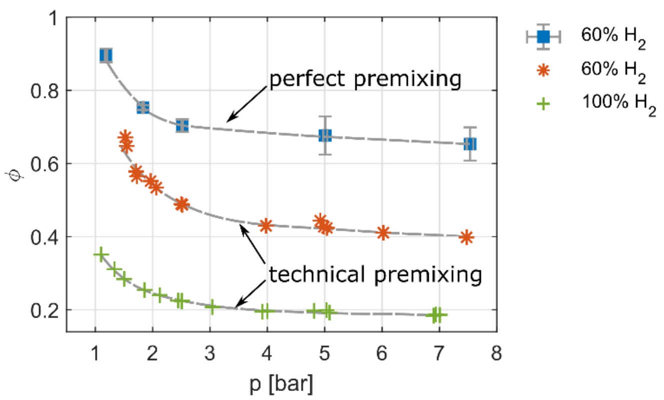

Figure 13: Effect of technical premixing on flashback limits at various pressures

6 Overall characteristics of flashback limits for CH_4/H_2 mixtures

The goal of this section is to give an overview on how flashback propensity of CH_4/H_2 mixture is affected by different parameters and operating conditions, such as pressure, p, preheat temperature, T_{pre}, bulk flow velocity, u_{bulk}, center body wall temperature, T_{wall}, and swirl angle. In particular, flashback propensity trends are analyzed at conditions relevant, for gas turbine combustors. The aim is to get an insight into how much hydrogen can be added to methane or natural gas without requiring major hardware modifications to state of the art gas turbine burner designs (here represented by a generic annular swirl burner configuration).

Figure 14 shows a summary of flashback limits for a range of preheat temperatures (200-400˚C), bulk velocities in the annular premix section (10-30 m/s), pressures (2.5 and 5 bar), hydrogen volumetric fractions in the fuel mixture (30-100%) and swirl flow angles (50˚, 55˚).

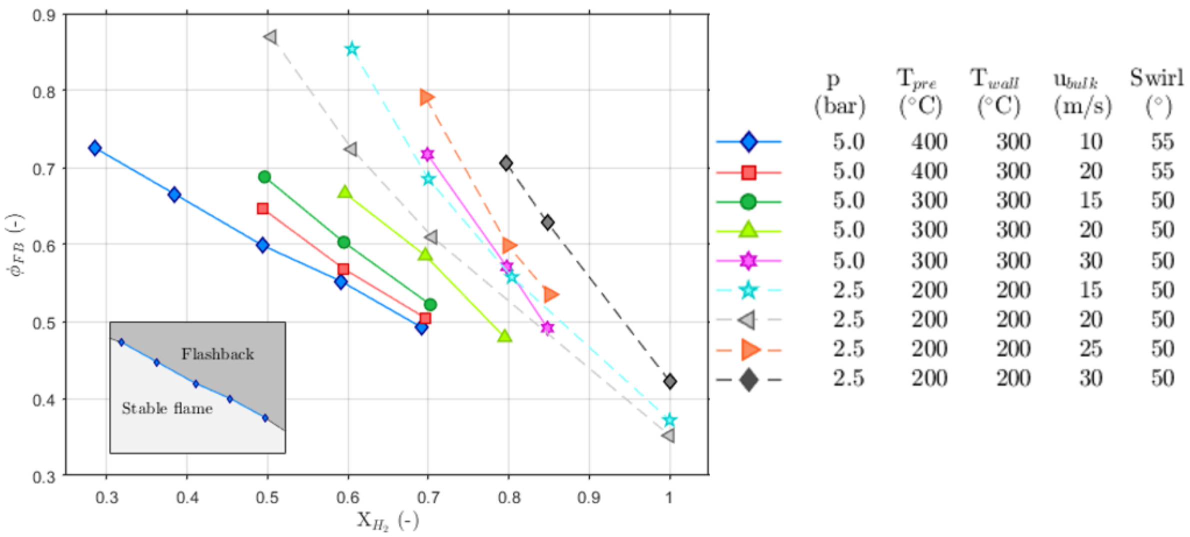

Figure 14. Flashback limits for different operating conditions at different hydrogen volumetric fraction in the fuel mixture.

The flashback limits are indicated as the equivalence ratio at which the flame front moves upstream into annular premix section (towards the swirler element). The region below each individual line represents stable operating conditions (flame is stabilized downstream of the annular premix section), above the flashback limit borderline no stable operation can be realized. From the trends shown in Figure 14, we can make some general considerations. Moving from low pressure and preheat temperature, to higher values, flashback occurs already at lower equivalence ratios (the flame is less stable). This could be related to the fact that turbulence flame speed increases with rising preheat temperature and flame thickness decreases with pressure. Both these parameters have traditionally been considered central to flame flashback understanding (Donohoe et.al., 2014).

In Figure 15, the effect of bulk velocity on flashback propensity can be addressed in more detail. The flashback limit data in Figure 16 were measured at the following experimental conditions: p = 5 bar, T_{pre} = 300˚C, T_{wall} = 300˚C, swirl angle = 50˚. Consider an hydrogen volumetric content of 70%. At these conditions flashback occurs at φ about 0.52 for the 15 m/s curve, φ = 0.58 and 0.71 for the 20 and 30 m/s bulk velocity curves respectively. As we move towards (only slightly) higher hydrogen concentration in the fuel mixture (80% vol.), the flashback limits shift to (significantly) lower equivalence ratios, phi = 0.48 for the 20 m/s curve and phi = 0.57 for the 30 m/s, showing, similarly to the pressure and preheat temperature effect, that higher flame speed and lower flame thickness lead to higher flashback propensity.

Furthermore, comparing two fixed hydrogen concentrations, the flashback limits difference between the bulk velocity curves drops from low to high hydrogen concentration. As we approach 100% hydrogen concentration in the fuel, the effect of bulk velocity on the flashback limits gets weaker. The mixture property change, due to hydrogen addition, alters the interaction between the turbulence flow field and the flame front. The decreased boundary layer thickness, associated with higher bulk velocities, makes the flame more resistent to flashback. However, towards high hydrogen concentration, this effect seems to be more than compensated by the flame thickness reduction. Figure 15 also includes a contour map of adiabatic flame temperatures obtained from one-dimensional, adiabatic free flame simulation using Cantera (Goodwin et.al., 2018). The AramcoMech 1.3 chemical mechanism was used, since this mechanism shows good performance when used to compute laminar flame speed data of lean CH_4/H_2 flames (Metcalfe et.al., 2013; Donohoe et.al., 2014). The two black dotted lines in the colormap show a temperature range relevant for state of the art gas turbine combustors Turbine Inlet Temeprature (TIT). According to this diagram, a volumetric hydrogen fraction of almost 70% could already be achieved in modern gas turbine combustors without leading to flashback.

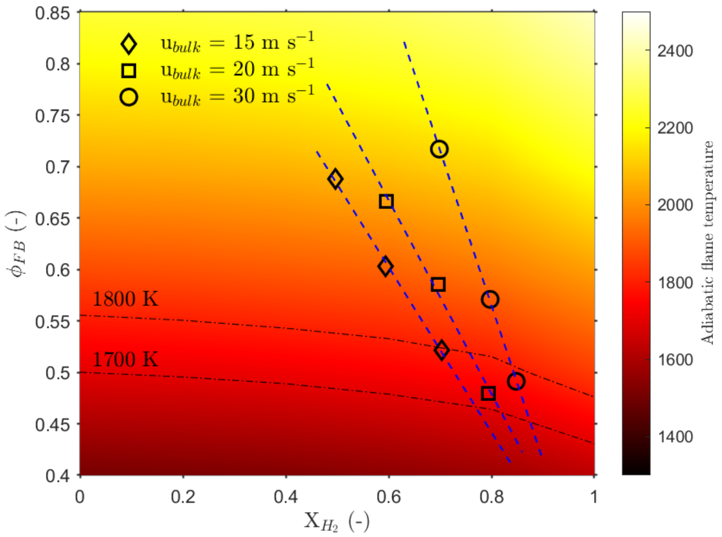

Figure 15. Flashback limits of different bulk flow velocities, as function of hydrogen volumetric fraction in the fuel mixture at p = 5 bar, T_{pre} = 300˚C, T_{wall} = 300˚C, swirl angle = 50˚.

Figure 16 shows the effects of technical and perfect premixing on flashback limits. To achieve “perfect” premixed conditions, fuel injection occurs significantly upstream of the swirler component and a static mixing device is used. For “technical” premixed conditions, the fuel is injected into the air passage of the swirler. Therefore, the mixing occurs exclusively in the annular channel of the combustor. Consequently, the flow is characterized by some unmixidness, which is also commonly found in typical gas turbine burners. In non-perfect premixed conditions, local variations of equivalence ratio are found (equivalence ratio stratification; local volumes of fuel lean/rich composition). Modern combustor design aims to minimize these local equivalence ratio variations, because they are responsible for higher pollutant (NOx) emissions. The diagram clearly shows that flashback propensity is much higher at “technical” premixed conditions. This suggests that, when fuel richer/leaner flow structures reach the flame front, their interaction with the turbulent flow field can play a primary role in the onset of the instability. Similarly, to Figure 15, Figure 16 shows the adiabatic flame temperature color map (typical modern gas turbine TIT highlighted in green). The diagram indicates that, in case of local equivalence ratio fluctuations state of the art gas turbine combustor would encounter high-risk flashback scenarios already at around 50% H_2 concentration in the fuel mixture. This is in contrast with the results shown in Figure 15, where high-risk H_2 concentration values were shifted to 70% or 80%. Even in light of these unmixedness effects, it still looks feasible to introduce a hydrogen concentration up to 30% without the need for major combustor hardware modifications.

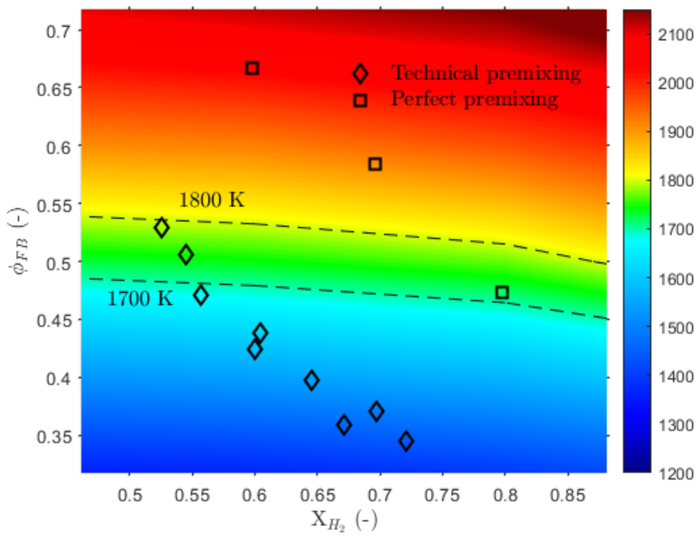

Figure 16: Perfect and technical premixing flashback limits (p = 5 bar, T_{pre} = 300˚C, u_{bulk} = 20 m/s), as function of hydrogen volumetric fraction in the fuel mixture.

7 Large Eddy Simulation of Flashback in the PSI swirl burner configuration

7.1 Computational Configuration

In this section, Large Eddy Simulation (LES) of the PSI turbulent swirl burner are presented. The computational configuration closely mimics the experimental test rig, consisting of an upstream annular tube with outer radius $r = 18.35$ mm and inner radius $r = 9$ mm and axial length of $x = 195$ mm that represents the mixing section, and a downstream cylinder of radius $r = 37.5$ mm and length $x = 95$ mm representing the combustion section. Eight equally spaced swirler vanes connecting the inner wall to the outer wall are present at the start of the mixing section with trailing angles of 50° and 65° considered in the current work.

The LES in this work were performed using the compressible reactive code AVBP (Gicquel et al., 2011). Subfilter turbulence closure was achieved with the dynamic Smagorinsky model (Germano et al., 1991) while Subfilter closure of chemical source terms was achieved with the dynamically thickened flame approach (Colin, 2000). A detailed hydrogen mechanism with nine chemical species and nineteen reactions was used to model chemical reactions (Li, 2004). The diffusivity of each individual chemical species was modeled with a constant, non-unity Schmidt number.

The mesh used to discretize the domain has a characteristic length of 0.5 mm throughout the entire mixing section, except near the inner wall where this decreases to a characteristic length of 0.2 mm. This corresponds to a length of approximately $y^+ = 10$ near the wall. Because confined flashback (i.e., where the flame already protrudes into the mixing section before flashback) is the main interest in this work, a coarser grid is used in the combustion section.

The simulation domain and its boundary conditions are shown Figure 17. A bulk inlet velocity of 30 m/s corresponding to the experiments is used. Perfectly mixed pure hydrogen-air mixtures are assumed for all reactive cases, while pure air is assumed for all nonreactive cases. Inlet temperatures of 473 K and outlet pressures of 2.5 bar are used in all simulations, again corresponding to experiments. Because the boundary layer is not fully resolved, wall-models (Van Driest, 1951) are applied at all solid boundaries. All walls are treated as adiabatic, except for the inner wall of the mixing section which is treated as isothermal (to match oil cooling present in the experiments) at a prescribed temperature of 473 K.

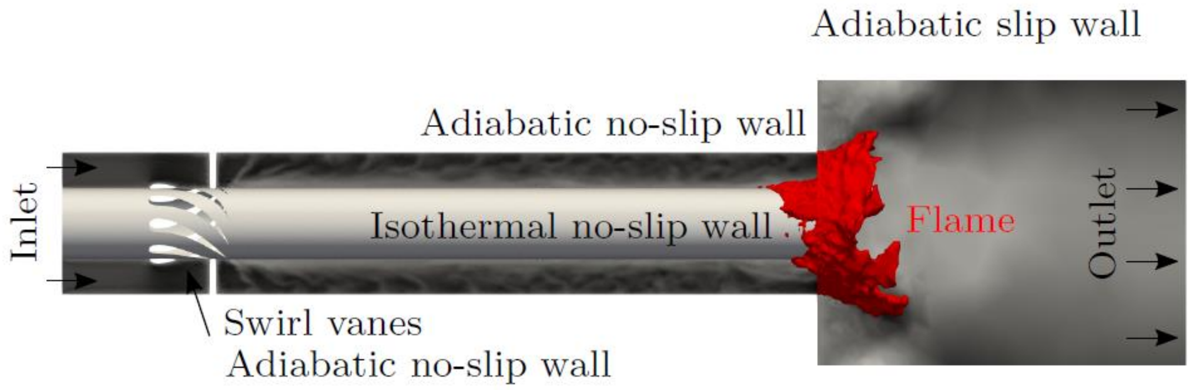

Figure 17: Boundary conditions and domain for the LES in the present work.

Two different swirl angles are considered in this work based on interesting conditions identified experimentally. For each swirl angle, simulations are performed at equivalence ratios just below the flashback limit (stable), just above the flashback limit (flashback), and for a single non-reacting case. Note that the goal of these simulations is to better understand unanswered questions from the experimental portion of the campaign, as well as to better inform models meant to predict flashback. Therefore, capturing the exact flashback limits (which would require enormous resources to fully resolve the flame and flow near the wall) is not the goal.

7.2 Validation and comparison with experiments

When recording flashback limits in the PSI burner, equivalence ratios are slowly increased until flashback occurs. Even before the onset of flashback, the flame already protrudes into the mixing section to some degree. However, the flame does not continue to propagate and is therefore not globally considered flashback. Eventually, the equivalence ratio is increased sufficiently high that true, global flashback occurs such that the flame rapidly propagates along the entirety of the mixing section. The flashback limit can then be identified as the value of the equivalence ratio where this occurred.

Mimicking this process computationally is unfeasible because of the extremely long simulation timescales needed for a sufficiently slow increase in equivalence ratio. Instead, the present work increases the equivalence ratio in discrete quantities of 0.025. The simulation proceeds for long enough to ensure that flashback will not occur before the equivalence ratio is again increased. This process is continued until flashback occurs.

The simulated flashback limits are compared to experimental measurements in Table 2. The predictions are reasonable, especially for larger swirl angles. However, given the lack of near-wall resolution, there is no expectation of extreme accuracy. In addition, flashback limit trends with changing angles are captured even in this relatively coarse simulation.

Table 2: Simulated and experimental flashback limits for different swirl vane angles

Angle	ϕ_{exp}	ϕ_{sim}
50°	0.42	0.300
65°	0.31	0.275

To better understand flashback, the leading point of the simulated flames is studied. This is defined as the point on the $T = 750$ K iso-contour with the smallest axial location (i.e., closest to the inlet). The behavior of this point is shown for both swirl angles both at a stable and flashback equivalence ratio in Figure 18. In both cases, the flame clearly protrudes into the mixing section (i.e., $x < 195$ mm) even before the onset of flashback. At these conditions, the leading point of the flame is relatively stationary both axially and azimuthally for low swirl angles. However, the leading point of the flame rotates around the inner wall in the direction of the flow for the high swirl angles. Upon changing the equivalence ratio above the flashback limit, both flames propagate forward. A significantly larger axial velocity is recorded for the high swirl angle case. Interestingly, the high swirl angle case continues to rotate with the direction of the flow during flashback, whereas the low swirl angle rotates in the opposite direction, *against* the direction of the swirling flow.

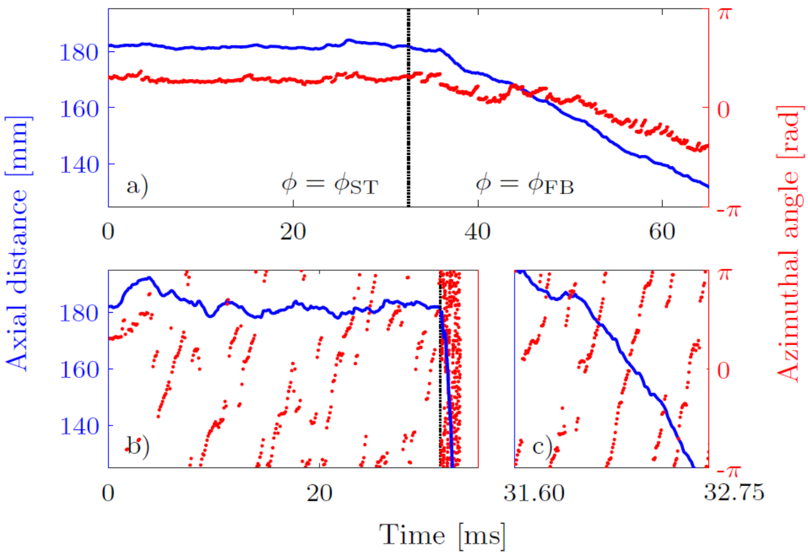

Figure 18: Axial distance from the inlet (blue) and azimuthal angle (red) of the leading flame point over time for both the 50 (a) and 65 (b) degree cases. Vertical dashed lines indicated the transition from a stable equivalence ratio to a flashback equivalence ratio. The inset (c) shows a temporally-zoomed view of the 65 degree case after transition to flashback.

This rotation is perfectly consistent with what has previously been observed experimentally at PSI during this project. Specifically, both experiments and simulations capture counter-swirl propagation for the 50° case, and co-swirl propagation for the 65° case. A qualitative comparison of this behavior both experimentally and computationally is shown in Figure 19. The major qualitative differences between the two flame propagation modes are highlighted, showing a flame at low swirl flame propagating against the direction of swirl and a high swirl flame propagating with the direction of swirl. Such a comparison indicates that the present simulation strategy is capable of sufficiently capturing important flashback behavior, even if the exact flashback limits are not captured.

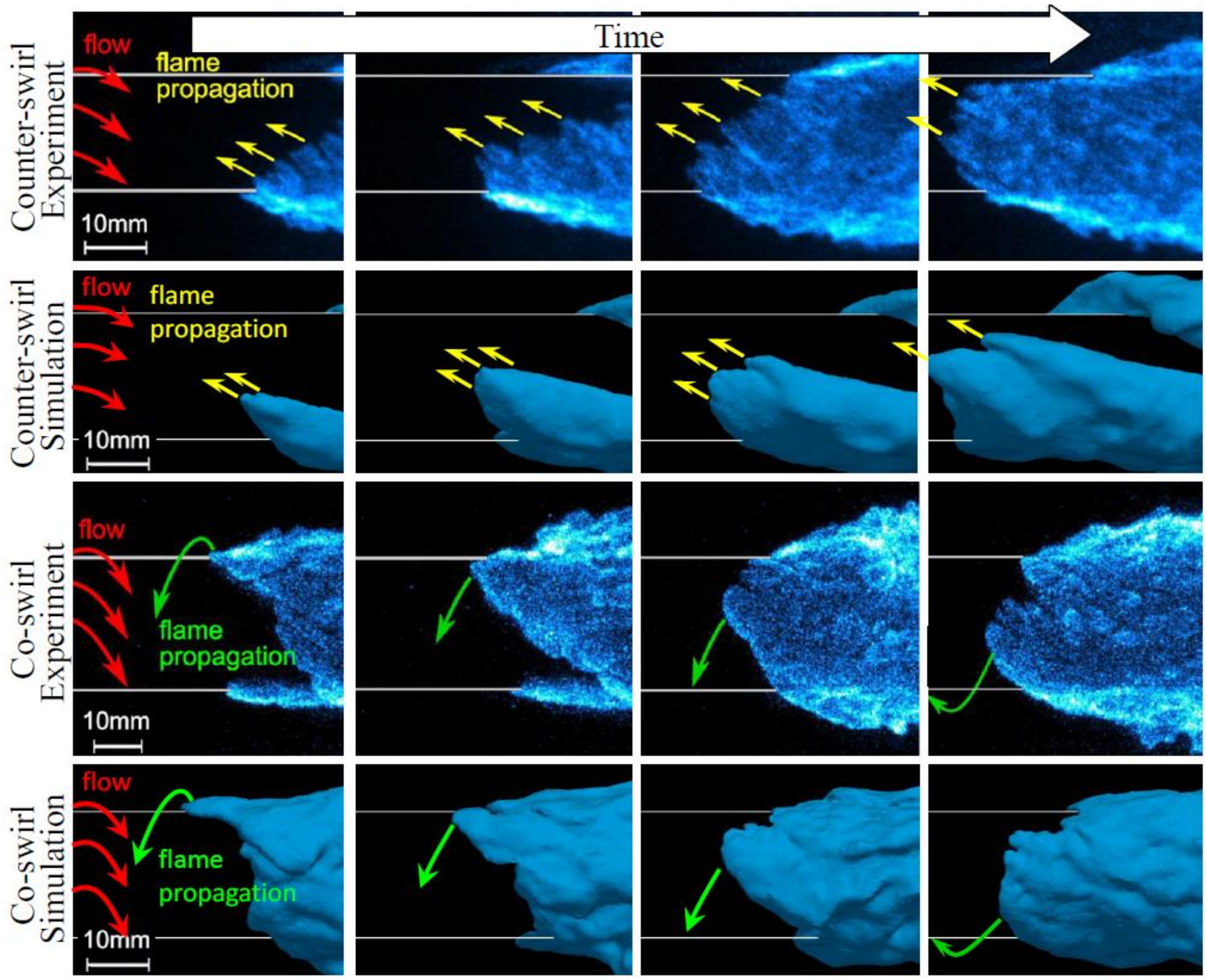

Figure 19: Qualitative comparison of the two rotational modes in experiments and simulations. The simulated flame is visualized using the T = 750 K iso-contour whereas the experimental flame is visualized using chemiluminescence.

The simulations are further validated by exploring near-wall behavior of the flame. To that end, instantaneous snapshots of the flashback process near the wall are shown in Figure 20. Snapshots a) and b) show the low swirl case and visualize how the near-wall flame propagates against the direction of swirl. This is in contrast to snapshots d) and e), which show the high swirl case and visualize the near-wall flame propagation with the direction of swirl. In the low swirl case, the flame is primarily composed of a large flame tongue with multiple small-scale bulges, whereas in the high swirl case the flame contains a number of smaller flame tongues throughout. In addition, the figure indicates that there is generally a single leading flame point for the low swirl case, but potentially many competing leading flame points for the high swirl case.

Figure 20 also explains the relationship between the flame and the flow near the wall during flashback. Regions of negative axial velocity are rare in the low swirl case, generally occurring just upstream of the leading flame point. This differs from the high swirl case, where negative axial velocity exists along a significant portion of the flame front. Through closer examination of the leading flame fronts with overlayed velocity vectors (frames c and f), it becomes clear that the flame behavior resembles that previously described by Ebi and Clemens (Ebi et al., 2016). For the high swirl case, the flow is deflected in front of the flame into a swirling motion which causes negative axial velocities on the leeward side of the flame front. These regions of negative axial velocity ultimately play an important role in controlling the flashback process and have been an important focus in the boundary layer flashback community. In contrast, the low swirl case does not exhibit large scale swirling motion, but rather illustrates that the leading flame point appears to expand against the direction of flow to create a small region of reverse flow. This is exactly consistent with the behavior previously described for small-scale bulges on the windward of the flame during flashback (Ebi et al., 2016). Interestingly, that earlier work identified these bulges as participating, but not dominating the flashback process, whereas the current work identifies conditions where these bulges are in fact the dominant flashback process as they are capable of counter-propagating against the flow.

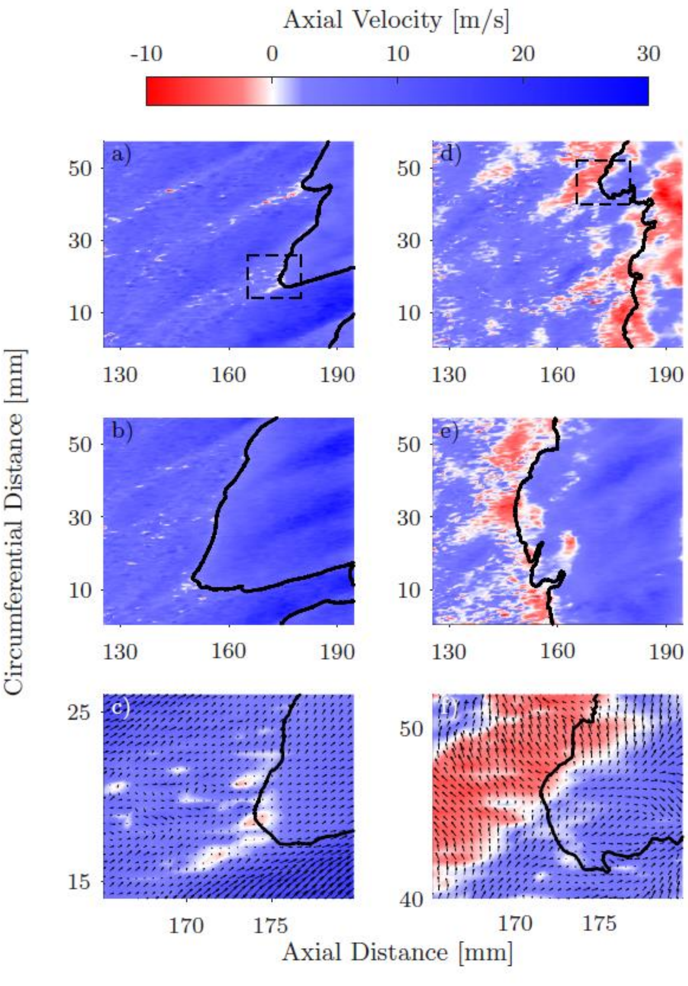

Figure 20: Instantaneous snapshots of flame front (black curve) and instantaneous axial velocity field (color) taken 0.2 mm from the central wall. Snapshots a) and b) show the low swirl case 30 ms apart, whereas d) and e) show the high swirl case 10 ms apart. Frames c) and f) provide a zoomed in view of a) and d), respectively, as indicated by dashed boxes.

7.3 Flashback flame dynamics

Given the previously shown qualitative agreement between simulations and experiments, two interesting points are now studied using the LES results. First, while the differing leading flame point behavior was identified at different swirl angles, it remains unclear what physical mechanism controls this behavior. Second, the simulations provide an abundance of data with which flame behavior near the flashback limit can be studied to help improve flashback limit models. In both cases, the simulations provide an opportunity to better understand flashback through quantities difficult to measure experimentally.

A better understanding of the two flame propagation modes is achieved by considering the non-reactive mean flow field to isolate the fluid dynamics at play. Both the axial and azimuthal components of velocity taken 0.2 mm from the wall are shown in Figure 21. Temporally stationary flow structures of low azimuthal order caused by convective instabilities are immediately obvious in the near-wall flow. These instabilities are not simply a result of downstream wakes from swirler vanes (e.g., there are eight swirlers, but less wakes) and qualitatively do not change with grid refinement.

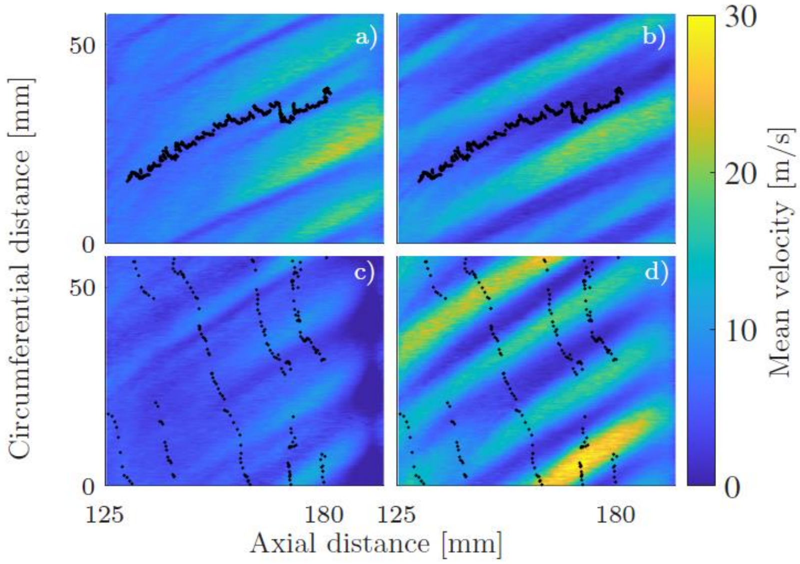

Figure 21: Non-reacting mean axial velocity (left) and mean azimuthal veocity (right) taken 0.2 mm from the central wall. The low swirl case is shown on the top, and the high swirl case is shown at the bottom. The location of the leading flame point from reacting simulations is shown every 0.1 ms as black points.

These instabilities lead to significant differences between the maximum and minimum velocities near the wall. For example, in the low swirl case, there is a difference of approximately 20 m/s between the smallest and largest values of axial velocity, which is expected to have a significant effect on flashback. The importance of these peaks and valleys in the velocity field on flashback is illustrated by overlaying the coordinates of the leading flame points during flashback at multiple instances of time over the velocity field in Figure 21. For the low swirl case, the leading flame point motion directly follows a low velocity region of the instability during flashback while completely avoiding high velocity regions. This differs from the high swirl case, where the leading flame point is shown to largely ignore the instability as it proceeds to rotate in the direction of swirl, mainly due to the significantly smaller difference between maximum and minimum velocities that develop at this swirl angle.

These near-wall flow instabilities have a major effect on boundary layer flashback and were shown in this work to specifically be the reason for the two different flame propagation modes at different swirl angles. Understanding how to control and suppress the instabilities is thus likely important for delaying flashback in practical burners. It is worth noting that the instabilities appear to grow stronger with axial distance in the mixing section, implying that short mixing sections are preferable to longer sections with respect to the instability and flashback.

The simulations are next leveraged to better understand flame behavior just before and after the flashback limit to aid in the design of predictive models. The present simulations are relatively novel in that there are few studies exploring the flame at equivalence ratios immediately around the flashback limits. It is expected that understanding changes in the flame dynamics across the flashback limit is important for better models. To provide such information, the joint probability density function of the local instantaneous axial flow velocity and axial flame displacement speed at the leading flame point at many different instants are shown in Figure 22. The figure illustrates that the behavior in all four cases (i.e., two swirl angles, before and after flashback) varies significantly. In particular, there is a significant difference in the probabilities of leading flame point behavior in each of the four visualized quadrants. This is important as each quadrant corresponds to significantly different behavior as summarized in Table 3.

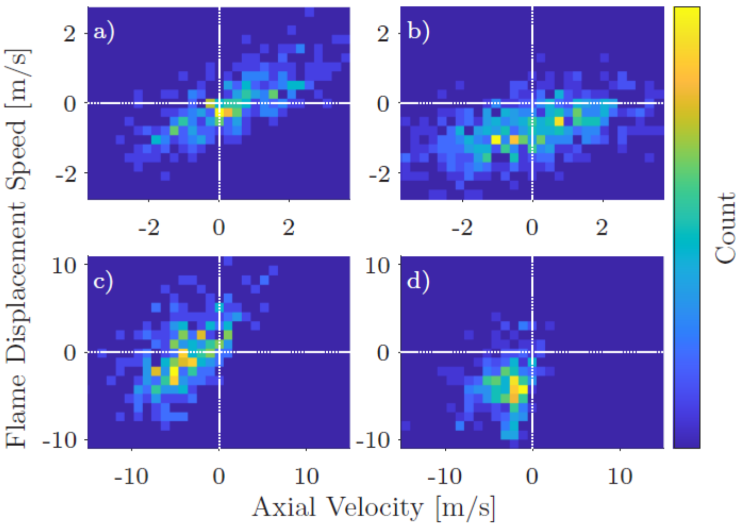

Figure 22: Joint probability density functions of the local instantaneous axial velocity and the local instananeous flame displacement speed at the leading flame point just below (left) and above (right) the flashback limit for the low swirl (top) and high swirl (bottom) cases. Negative flame speeds indicate flame motion towards the inlet.

Table 3: Dynamics of quadrants in Figure 22

Q_{II} Receding flame Negative axial velocity	Q_{I} Receding flame Positive axial velocity
Q_{III} Advancing flame Negative axial velocity	Q_{IV} Advancing flame Positive axial velocity

For low swirl below the flashback limit, data is primarily in quadrants 1, 3 and 4. The prevalence of points in quadrants 1 and 3, along with the near unity slope of data, indicate that the flame is largely flow controlled for this case (i.e., the flame moves forward with negative axial velocity, and backwards with positive axial velocity). However, there are a significant number of points in quadrant 4, which indicates points where the flame speed was sufficient to overcome the locally positive axial velocity.

For low swirl above the flashback limit, data is primarily in quadrants 3 and 4. This differs from the stable case, with many points from quadrant 1 shifted instead to quadrant 4, indicating that the flame speed is generally sufficient to overcome the flow speed.

For high swirl below the flashback limit, data is primarily in quadrants 2 and 3. This differs dramatically from the low swirl case in that there are few points in the right two quadrants, indicating that the leading flame point generally only experiences negative axial velocities. It is important to note that although this flame experiences very few instances of positive axial velocity, the flame is still globally stable (i.e., it propagates equally forward and backwards overall such that flashback does not occur). The data in quadrant 2 represents this motion towards the outlet, even with positive axial velocity. Such behavior is likely due to local flame extinction, which was previously identified as an important factor in boundary layer flashback during the experimental portion of the present study at PSI. It is hypothesized that the leading flame point propagates forward through negative axial velocities caused by flame expansion until it reaches a region of high stretch due to turbulence that causes local extinction and recedes the flame front.

For high swirl above the flashback limit, data is primarily in quadrant 3. The lack of points in quadrant 2 indicates that at the flashback equivalence ratio, the flame extinction stretch limit is now above the stretch it experiences in the flow, such that it can propagate without local flame extinction. Thus, the flame generally propagates forward and usually experiences negative axial velocity.

8 Improved model for flashback limit prediction in swirling flows

8.1 Background

Modeling boundary layer flashback first requires an understanding of the fundamental flame and flow balances relevant to the process. A simple overview of these processes is shown in Figure 23. Far away from the wall, the axial velocity of the flow is significantly larger than the flame speed, making propagation impossible. Very close to the wall, heat losses dominate, and the flame speed is therefore significantly decreased such that propagation is also impossible. Thus, there exists only a narrow band a small distance away from the wall where boundary layer flashback can occur.

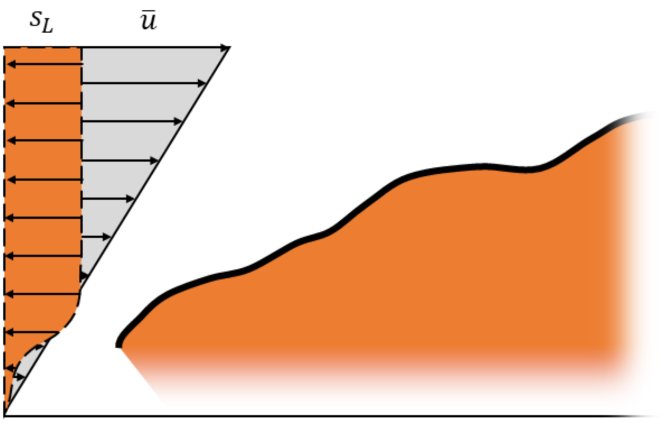

Figure 23: Illustration of boundary layer flashback. On the left, flame speed as a function of wall distance (orange) is laid over a near-wall velocity profile (gray) to show the small region where the flame can propagate forward. Dashed line indicates where flashback occurs.

Many models for describing flashback already exist. However, attempts at applying existing boundary layer flashback models to the present configuration have not resulted in the successful prediction of flashback limits, both in a quantitative, but also qualitative sense. The most fundamental boundary layer flashback model developed by Lewis and von Elbe (Lewis and Von Elbe, 1943) relies on the concept of a critical gradient, which balances the wall velocity gradient (g) and the unstretched laminar flame speed (s_L). When applied to non-swirling unconfined systems, the model collapses all flashback limits to a single value. However, practical gas turbines generally employ swirling flows which lead to confined flames. As shown in Figure 24, applying the model of Lewis and von Elbe to the flashback limit measurements from the present experimental campaign leads to neither a collapse of all data to a single constant, nor even to a collapse between data at different inlet velocities, indicating that the model is invalid at the practical gas turbine conditions in this work.

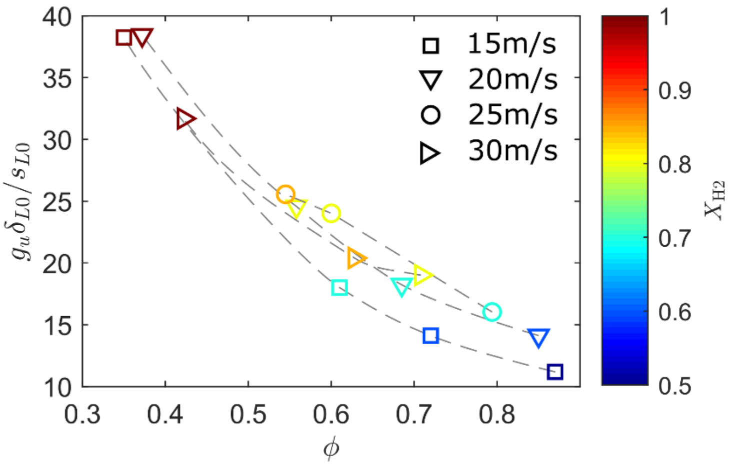

Figure 24: The model of Lewis and von Elbe applied to flashback measurements taken at the Paul Scherrer Institute. Each curve represents data taken at different bulk inlet velocities, while color represents fuel hydrogen content.

More recently, a model for boundary layer flashback limits was developed by Hoferichter et al. at the Technical University of Munich (Hoferichter et al., 2016), based on the idea of reversed flow in front of the flame due to the flame's own expansion. Theory describing boundary layer separation, flame pressure rise, turbulent burning velocity with weak stretch, and turbulent velocity fluctuations was combined to provide accurate prediction of flashback limits. The model was extremely successful in predicting flashback limits for atmospheric non-swirling hydrogen-air confined flames but was not previously used to predict flashback limits in more realistic conditions including swirl, natural gas/hydrogen mixtures, and higher pressures.

The experimental flashback limits measured at the Paul Scherrer Institute provided an opportunity to apply this model to a more practical gas turbine configuration. By extending the model to account for mixtures of hydrogen and methane, the experimentally measured flashback limits were compared to model predictions as shown in Figure 25. In its present form, the model is unable to accurately predict the experimentally measured flashback limits. Not only does the model underpredict the flashback propensity, but there is a wide spread of the experimental data at any given hydrogen content such that no qualitative trends can be studied.

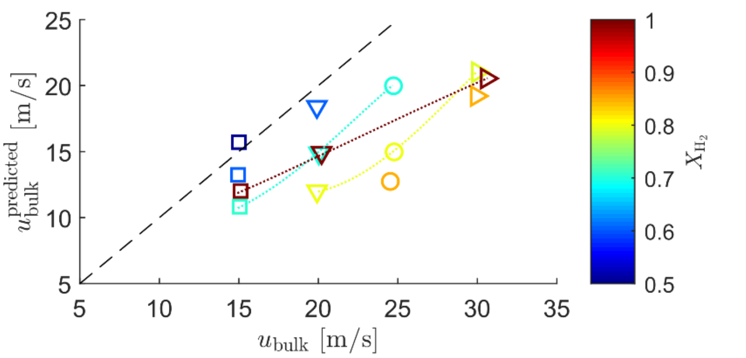

Figure 25: Flashback limits from the model developed at the Technical University of Munich compared to experimental measurements taken at the Paul Scherrer Institute. Markers indicate inlet velocity and color indicates hydrogen fraction.

While neither of the presented models are capable of accurately capturing the flashback limits of the presently studied configuration, a capable model remains an important tool for industry. In the next subsection, a new type of model is developed and presented that is capable of such predictions.

8.2 A critically strained flame model of boundary layer flashback

Examining the experimentally measured flashback limits from the swirling burner at the Paul Scherrer Institute, an important detail emerges. For a single inflow velocity, the extinction strain rate of a one-dimensional strained flame at the flashback thermochemical condition (i.e., temperature, pressure, and flashback equivalence ratio) remains constant. This is illustrated in Figure 26, where this strain rate, as well as a similar inverse time scale constructed from the strained flame speed and flame thickness are shown as a function of hydrogen content. Regardless of the amount of hydrogen in the fuel or the flashback equivalence ratio, these timescales remain constant, changing only with the bulk inflow velocity (a). Computing the same timescale for an unstretched flame at the same thermochemical conditions does not lead to similar behavior (b), indicating that strain-extinct flames may be important for modeling boundary layer flashback.

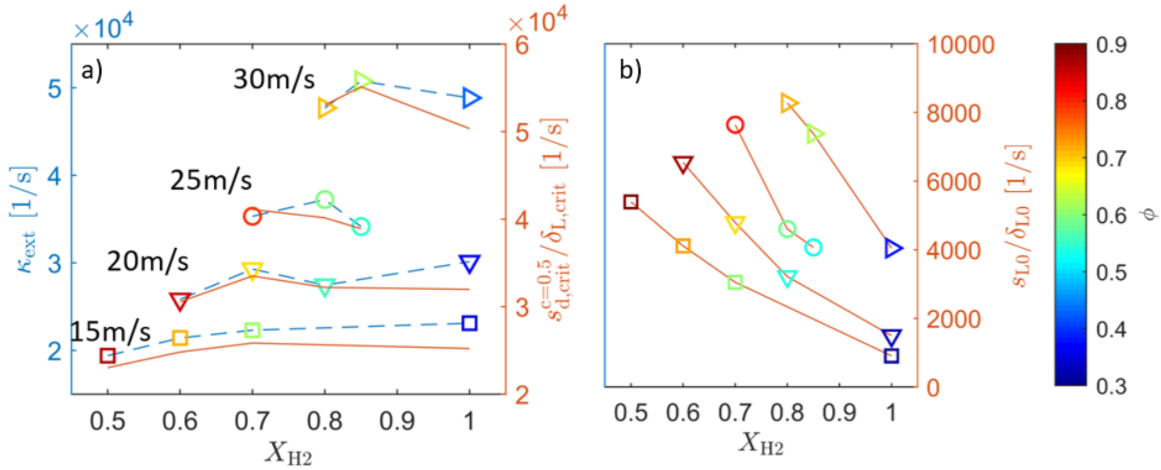

Figure 26: Inverse flame timescales at four bulk inlet velocities for stretched flames at the extinction limit (a) and unstretched flames (b).

While previous models have focused on the balance between flow and flame speed, the choice of flame speed has either been an unstrained flame speed (Lewis and Von Elbe) or a weakly stretched flame speed (Hoferichter et al.). However, Figure 26 instead indicates that a highly strained flame near the extinction limit may provide the correct flame speed (i.e., $\boldsymbol{s_{L,ext}}$). Since the flame propagates very close to the wall (i.e., within the linear sublayer of the boundary layer), the velocity profile is assumed to be linear and given by

$$\boldsymbol{u}^{+} = \boldsymbol{y}^{+},$$

where $\boldsymbol{u}^{+}$ is the viscous normalized velocity and $\boldsymbol{y}^{+}$ is the viscous normalized distance from the wall. With a linear velocity profile, the axial velocity gradient is equal to the value at the wall ($\boldsymbol{g}$). Then, the "critical" distance from the wall where the velocity matches the relevant flame speed is given by

$$\boldsymbol{d_c} = \frac{\boldsymbol{s_{L,ext}}}{\boldsymbol{g}}.$$

In addition, a thermal distance is also introduced to normalize the critical distance and is given by

$$\boldsymbol{d_t} = \sqrt{\frac{\boldsymbol{\alpha}}{\boldsymbol{g}}}$$

where α is the thermal diffusivity of the mixture. For a given temperature and pressure, the flame speed and thermal diffusivity are mainly functions of equivalence ratio, which is then a controlling parameter with the wall velocity gradient. The relationship between the critical distance, thermal distance, and the flashback limit remains unknown. To help close this relationship, non-swirling confined flashback limits from the Technical University of Munich (Eichler, 2011) are studied. These flashback limits are measured at atmospheric pressure, but across a large range of temperatures and equivalence ratios. Each measurement is reported as a flashback equivalence ratio and wall velocity gradient, and therefore can be used to compute a critical distance and thermal distance. Note that three different locations within the flame for computing the thermal diffusivity are tested: in the unburned mixture, the burned mixture, and near the center of the flame where the temperature gradient is maximum.

The value of the critical distance normalized by the thermal distance for all three values of the thermal diffusivity are shown in Figure 27. When the unburned or burned thermal diffusivity are computed, the data does not collapse. However, considering the thermal diffusivity taken near the center of the flame, all the data across all temperatures and equivalence ratios collapses to a constant value of unity. Physically, this implies that the critical distance is in fact equal to the thermal distance, as defined above. From a modeling perspective, this allows for a predictive model to be developed based on the equality of these two quantities.

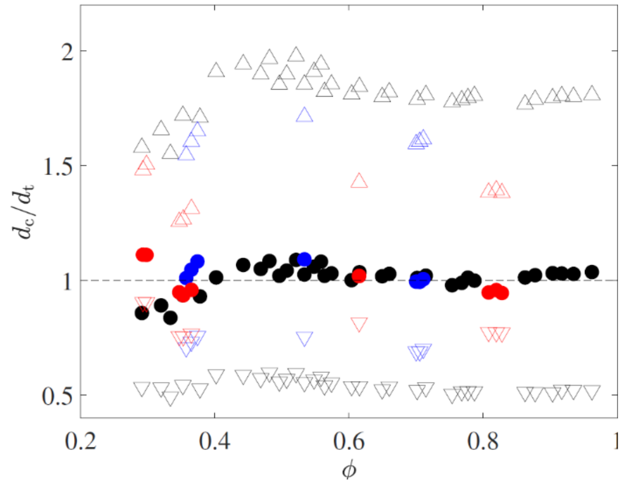

Figure 27: Critical distance normalized by thermal distance. Upward facing triangles indicate unburned thermal diffusivity, downward facing triangles indicate burned thermal diffusivity, and circles indicate thermal diffusivity near the flame center. Preheat temperatures of T = 20°C are indicated by black, T = 200°C by blue, and T = 400°C by red.

Equating the critical distance and thermal distance and rearranging leads to a simple equation governing boundary layer flashback:

$$\frac{s_{L,ext}^2}{\alpha g} = 1$$

As before, this equation contains a flame speed and thermal diffusivity, both controlled by the thermochemical state (e.g., equivalence ratio, preheat temperature, pressure, fuel composition) and the wall velocity gradient, presumably controlled mainly by the inflow velocity and burner geometry. Solutions to this equation give the flashback limits as a function of both the flow state and the thermochemical state. This is demonstrated in Figure , where the solutions to the model equation are computed and compared directly to the experimental data taken at the Technical University of Munich.

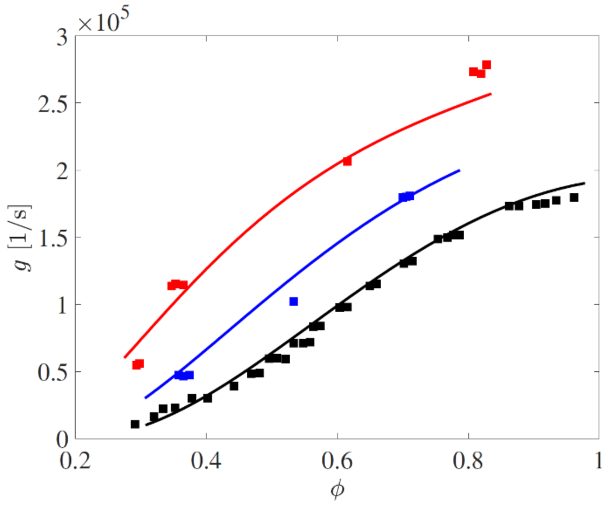

Figure 28: Modeled flashback limits compared to non-swirling experimental measurements. Preheat temperatures of T = 20°C are indicated by black, T = 200°C by blue, and T = 400°C by red.

As indicated in Figure , the newly developed model is capable of highly accurate flashback limit predictions in non-swirling flows. However, extension of this model to swirling flows with variations in hydrogen content is critical. Accounting for different fuels requires a trivial modification, as it is merely an alteration of the thermochemical state. As mentioned earlier, this simply affects the flame speed and thermal diffusivity through calculation of the one-dimensional strained flames. Unfortunately, extension to swirling flows is more difficult because this affects the axial wall velocity gradient. While this quantity is relatively simple to model in the non-swirling case, it can be significantly harder to model for the swirling case because it is a strong function of the swirler geometry. In order to maintain the role of the swirler geometry, the current model is extended to swirling flows by directly utilizing experimental measurements taken in the geometry of interest. Specifically, the model can be reversed to find the value of the wall velocity gradient which gives a modeled flashback limit that matches a single experimental flashback measurement (g_c). Specifically, given an experimentally measured value of the flashback limit ϕ_{FB}, the "controlling" wall velocity gradient can be computed as

$$g_c = \frac{s_{L,ext}^2(\phi_{\mathrm{FB}})}{\alpha(\phi_{\mathrm{FB}})}$$

As mentioned previously, this wall velocity gradient is expected to be a function mainly of the inlet velocity and geometry. Thus, the value extracted using the experimental measurement alongside the model should remain valid even as temperature, pressure, hydrogen content, etc. change, so long as the inlet velocity and geometry remain unchanged. This can be extended even further by assuming that, for a constant geometry, the wall velocity gradient will change linearly with the inlet flow velocity. Then, a single experimental measurement combined with the model should be able to predict the flashback limits within a given combustor even with changes in the thermochemical and flow conditions. This is illustrated in Figure 29, where the flashback limits predicted by the present model (combined with one experimental measurement) are compared to the swirling flashback limits measured experimentally at the Paul Scherrer Institute.

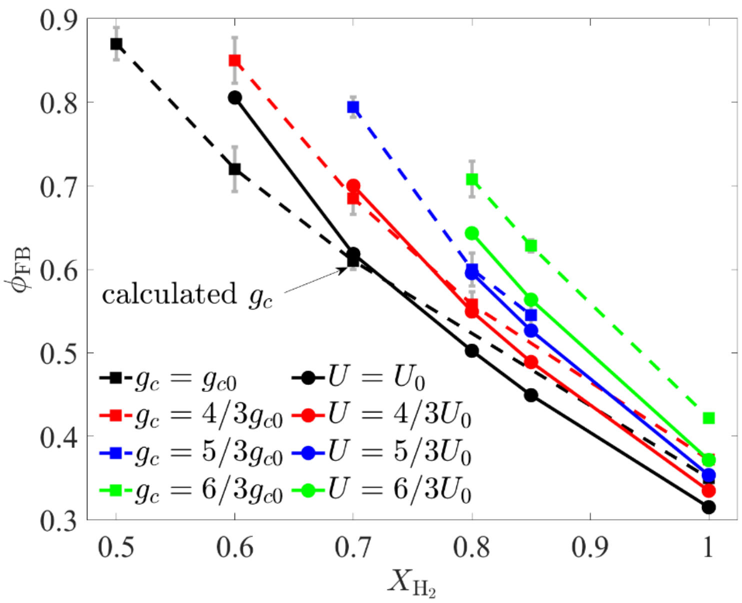

Figure 29: Model flashback limits (solid lines, circles) compared to those experimentally measured in a swirl burner at the Paul Scherrer Institute (dashed lines, squares) as a function of hydrogen addition to the fuel. Each color represents a different inlet velocity. The experimental point used to infer g_{c0} is indicated by an arrow. Flashback measurements are taken at T = 200 °C, and P = 2.5 atm.

Based on Figure 29, this combined model/experiment procedure is capable of accurately and affordably capturing both the quantitative flashback limits and the qualitative trends. In order to show that the model is applicable even in the conditions expected for next-generation gas turbines, flashback limits are predicted and compared to experimental measurements at elevated pressures in Figure 30.

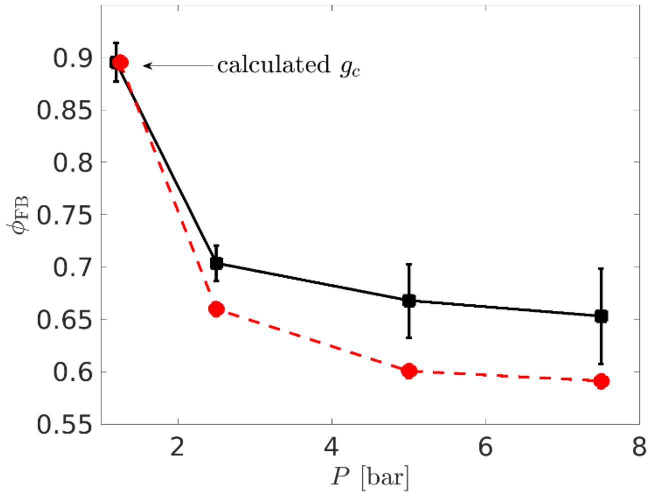

Figure 30: Model flashback limits (red dashed line, circles) compared to those experimentally measured in a swirl burner at the Paul Scherrer Institute (black solid line, squares) as a function of pressure. As before, the experimental point used to infer g_c is indicated by an arrow. Flashback measurements are taken at T = 200 °C, xH2 = 0.6, U = 20 m/s.

Again, the model closely agrees with the flashback limits measured at the Paul Scherrer Institute based on a single experimental measurement taken near atmospheric pressure. As identified in experiments previously, an increase in pressure decreases the flashback equivalence ratio down to a saturation limit, after which flashback propensity seems to be largely insensitive to pressure changes.

The model is also capable of exploring the flashback limit response as a function of changing temperatures in the system. Two temperatures are controllable in the PSI test rig: inlet temperature and inner wall temperature. The ability of the model to predict flashback limits while adjusting both temperatures together (i.e. inlet temperature identical to wall temperature) is shown in Figure 31. The figure shows that again, using a single value of controlling wall velocity gradient is sufficient for good model prediction of flashback limits at several other conditions. Notably, a single value of the controlling wall velocity gradient is sufficient to predict temperature changes even as the hydrogen content in the system changes as well. All qualitative trends are captured in this figure alongside good quantitative prediction of flashback limits.

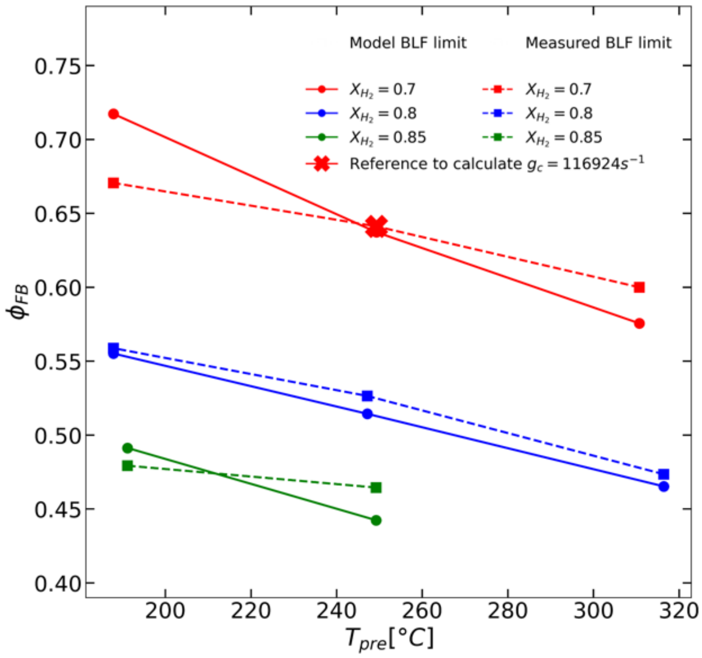

Figure 31: Boundary layer flashback limits as a function of temperature at P = 5 atm and U = 20 m/s based on experimental data from PSI.

Next, the case of changing wall temperature separate from the inlet temperature is considered. While there exist two temperatures in the system, it is not immediately obviously which temperature should be used in the model. In fact, two factors need to be considered.

First, the existence of a temperature gradient between the wall and the freestream implies that the correct temperature for use in the model may need to be somewhere between the two extremes. However, given that the flame propagates very close to the wall during flashback, the temperature used in the model is likely, to first order approximation, just the wall temperature. It is expected that this assumption is valid especially for smaller temperature gradients but may be insufficient for large temperature gradients.

Second, large increases in temperature are expected to affect the flow in the boundary layer, such that a single controlling wall velocity gradient may not be sufficient to describe the system. This is examined in Figure 32, where the experimental measurements from PSI are shown over the value of g_c required for the model to predict the given flashback limit. Even across the large change in temperature, the experimental curve generally follows a relatively constant value of the controlling wall velocity gradient, indicating that the model would successfully be able to reproduce the flashback behavior of the system. However, it is worth noting that the required value of controlling wall velocity gradient is not perfectly constant, implying that the impact of the wall temperature on the boundary layer is relatively important and should be considered for better predictions of the flashback limits. The model is used to predict flashback limits in Figure 33, where it is again seen that qualitative trends are captured with decent quantitative accuracy. As mentioned, the effect of the wall temperature on the boundary layer does lead to a more strongly negative slope in the model than in the experimental data, but the model still provides quantitatively accurate information about the flashback limits.

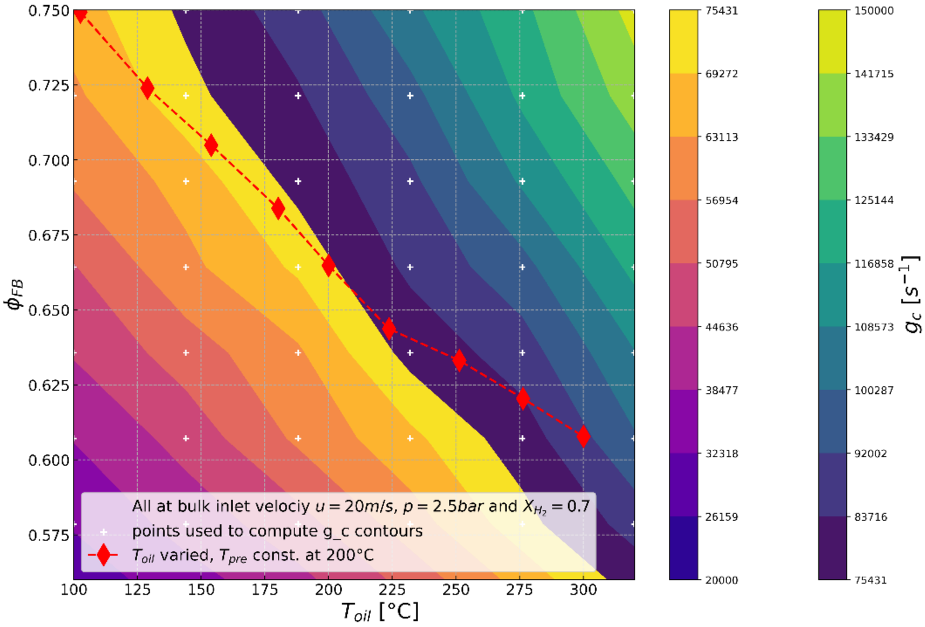

Figure 32: Experimentally measured flashback limits with changing wall temperature at a constant inlet temperature (red diamonds) shown over the value of the controlling wall gradient required for the model to predict a given flashback limit equivalence ratio (color field). An iso-contour of the color field implies that a single value of the wall velocity gradient is sufficient for the model to capture the experiments.

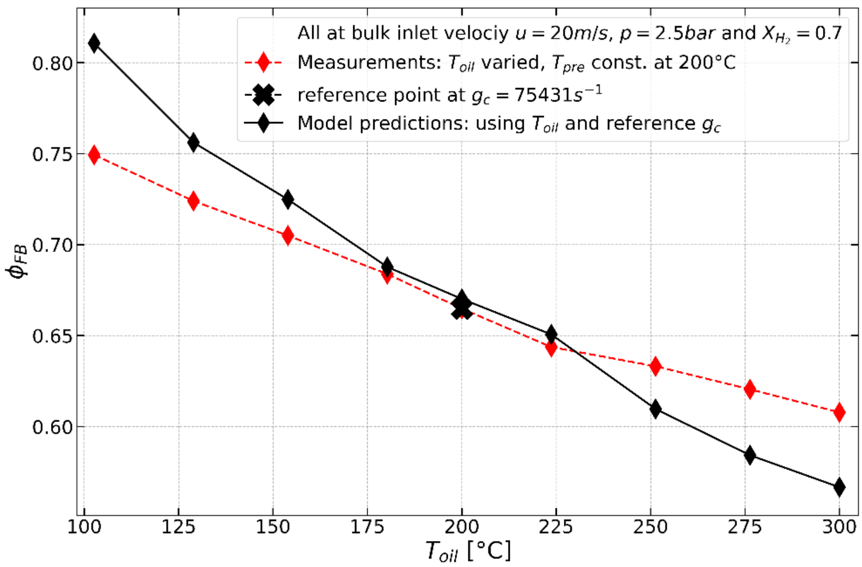

Figure 33: Experimentally measured flashback limits (red) compared to model predictions (black) as a function of the changing wall temperature. Note that the inlet temperature is kept constant.

9 Conclusions and Guidelines

Flashback limits have been investigated systematically for a wide range of conditions up to 7.5bar and 300°C preheat temperature. The effect of pressure, preheat temperature, hydrogen content, premix strategy, swirl and bulk flow velocity on the flashback limit has been quantified for well-controlled boundary conditions. The compiled database serves as validation data for a flashback prediction model developed in this project based on the improved detailed understanding of the physical-chemical mechanisms governing the propagation of a flame front near the wall (boundary layer flashbacks, BLFs) of a generic premix burner configuration.

High-speed chemiluminescence and planar-laser induced fluorescence imaging of the OH radical have been applied to study the flame propagation pathway and flame structure. The results show that two distinct flame propagation pathways exist in swirl flame boundary layer flashback, with swirl number being the dominant parameter distinguishing between the two propagation modes (at low swirl - flame propagates against the direction of swirl; at high swirl - flame propagates with the direction of swirl). Even though this creates vastly different local flow conditions around the leading edge of the flame front, no major difference can be observed in the corresponding flashback limits of low resp. high swirl flow. Hence, flashback events investigated in the current work (especially for low swirl) may conceptually be viewed as non-swirling boundary layer flashbacks (BLFs). This is an important finding because models developed for non-swirling BLF should then also be applicable for flashback events up to a swirl number of about 0.7.

Chemical kinetics computations of one-dimensional, stretched flames at the conditions of flame flashback have been conducted. The results show that at a fixed pressure of 2.5bar and 200° preheat temperature, flames across a wide range of hydrogen content and equivalence ratio all share a common critical stretch rate at the instant of flashback. This finding offers a pathway for improved models to predict a flashback limit.

The LES (Large Eddy Simulation) modeling in this work was performed using a compressible reactive code with subfilter models for turbulence and chemical source terms closure and a detailed hydrogen mechanism with nine chemical species and nineteen reactions. Mimicking the full flashback process computationally is unfeasible because of the extremely long simulation timescales needed. However, the onset of a flame propagating upstream can be captured by the LES modeling. These simulated flashback limits are reasonably close compared to the experimental measurements. In addition, flashback limit trends for various operating parameters are captured correctly. A detailed analysis of the computational results produces valuable additional insight into the relationship between the flame front and the flow conditions near the wall during flashback. The simulations provide an abundance of data with which the flame behavior near the flashback limit can be studied to help understand the underlying physical-chemical mechanisms. The simulations provide an opportunity to better understand flashback through quantities difficult to measure experimentally. With this enhanced knowledge basis improved flashback (limit) models can be developed.

Particle image velocimetry measurements have provided the velocity field in the premix section of the swirl burner. The velocity profiles serve as an input and validation data for all modelling activities. Examining the experimentally measured flashback limits from the swirling burner at the Paul Scherrer Institute, it became apparent that – at a given bulk flow velocity - the extinction strain rate of a one-dimensional strained flame remains constant at the given thermochemical conditions (i.e., temperature, pressure, and equivalence ratio) when flashback occurs.

As none of the flashback prediction models reported in literature is capable of accurately capturing the flashback limits of the presently studied configuration, a new type of model has been developed which proved to be actually capable of such predictions. Such a model remains an important tool for all kinds of combustion applications (especially for the gas turbine industry) and will be further developed in this direction.

The newly developed model is capable of highly accurate flashback limit predictions in non-swirling flows (literature data), as well as for swirling flows (this study). The model can be used to find the value of the critical wall velocity gradient at a given flashback event. This wall velocity gradient is expected to be a function mainly of the inlet velocity and geometry. Thus, the value extracted should remain valid even as temperature, pressure, hydrogen content, etc. change, so long as the inlet velocity and geometry remain unchanged. This can be extended even further by assuming that, for a constant geometry, the wall velocity gradient will change linearly with the inlet flow velocity. Then, a single experimental measurement combined with the model should be able to predict the flashback limits within a given combustor even with changes in the thermochemical properties (pressure, temperature, fuel composition, stoichiometry) and the flow conditions. If this can be confirmed for a few different burner geometries and flow conditions, the model might evolve as a mighty tool for flashback limit predictions.

In order to show that the model is applicable to various thermochemical conditions, flashback limits have been predicted and compared to experimental measurements at different pressure/temperature and fuel gas mixture conditions. Even across a large range in wall temperature, the model does successfully reproduce the flashback behavior of the system. As wall temperature plays an important role in controlling flashback events, this predictive capability of the presented model is of utmost importance. As a major recommendation based on the results achieved, a control of the wall temperature (at least in certain critical zones of the burner/mixer configuration) can be considered very effective for the suppression of the boundary layer flashback risk for fuel gas mixtures containing increasing amounts of hydrogen. To this extent a re-design of gas turbine burners seems (somewhat easily) feasible which should include active cooling of certain critical parts of the burner. The local cooling in this respect can be reasonably achieved with (inter-cooled) compressed air taken from the gas turbine compressor.

<u>Best practice design guidelines</u> (for premix gas turbine burners to be used with H_2 fuels)

- Minimize (avoid) low flow velocity zones, i.e. minimize boundary layer thickness (low swirl flow), energize boundary layers (film air, effusion cooling), avoid cavities in the premix section
- Lean-out low flow velocity zones (reduced fuel concentration in the near wall region/boundary layer) by proper design of the fuel injection and (optionally) additional film air injection (into boundary layers).
- Avoid fuel rich streaks (by proper design of the fuel injection) in combination with low flow velocity zones; strive for as perfect premixing of (H2) fuel & air as possible
- Control the wall temperature (at least in certain critical zones of the burner/mixer configuration) to a minimum value (target range: 200 – 250°C).
- Wall cooling, (extremely) fuel lean conditions and thin boundary layers can be achieved in a combined manner by application of design features such as film cooling or effusion cooling within the boundaries of the burner/premixer section
- A re-design of gas turbine burners (new design or retrofit) should consider active cooling (by air or water) of certain critical parts of the burner.
- Check the burner design (with numerical simulations) for critical zones during the design phase; apply a suitable flashback prediction model (e.g. the one developed in this project based on a critical strain rate criteria) to detect & correct design features prone for flashback.
- Check the burner design (with a few dedicated experiments) for flashback resistance, in order to validate the final design; with a proper flashback prediction model experiments need to be performed only at ambient/moderate pressure levels, and can be extrapolated to real gas turbine operating conditions.

10 Outlook and Follow-Up

The major learnings from the experimental work was the (re-)confirmation of the importance of the fuel/air mixing quality (i.e. distribution/spread of local equivalence ratios) and of the wall temperature in controlling the flashback limits of a given burner geometry.

As in the current work the mixing quality was only qualitatively defined by two distinctly different fuel injection locations & methods (perfect premixing = multi-point injection far upstream of burner exit; technical premixing = injection through multiple injection ports integrated in the swirler vanes), we are now following up this work with a quantitative characterization of the mixing quality resulting from these two fuel injection configurations. In an ongoing effort we currently do experimental work in a dedicated optically accessible test set-up measuring the mixing quality in quantitative terms based on laser induced fluorescence with acetone as a marker substance. These studies will further help in understanding the local conditions near/in the boundary layer, and will provide an additional data basis for validating the experimental flashback data.

In a further parametric study we will also continue to test the capabilities of the flashback limit prediction model with respect to its sensitivity towards variation of major operating parameters (pressure, preheat temperature, fuel composition, fuel/air stoichiometry). Possibly this study will be connected to different burner geometries/burner types in order to find out whether the model can be really used in order to qualify existing burner geometries with respect to their susceptibility for flashback when H_2 is introduced into the fuel mixture (focus: CH_4/H_2 mixtures).

In a similar way new unconventional burner geometries should be investigated, in order to prove that the predictive model can really be used in a meaningful way to guide burner design processes in the direction of burner geometries which effectively prevent flashback events (when operated with H_2 or H_2-containing fuel mixtures).

This should be supported by a follow-up experimental study proving the effectiveness of (local) wall cooling as a means to prevent flashback in given and future burner configurations (possibly at a wide range of operating conditions – including elevated pressure and air temperature – which are most relevant for future gas turbine engines run with H_2-rich fuel gas mixtures).

11 National and international cooperation

All LES-based modelling activities are done in cooperation with the CAPS Laboratory at ETH Zurich (Prof. Noiray).

Results of flashback limit measurements and analysis on models predicting flashback limits are exchanged with the Combustion Laboratory at the University of California, Irvine, USA (Prof. McDonell), one of the leading groups in the US for flashback limit investigations with a focus on gas turbines applications.

The findings and conclusions have also been reported and discussed within the IEA Technology Collaboration Program (TCP) on Combustion, Gas Turbine Task group. Members of the Gas Turbine Task group have been informed about the major outcome on a regular basis, and participants (country representatives and IEA officers) of the TCP have been briefed during Task Leaders Meetings on a yearly schedule.

12 Publications

Jansohn, P. & Ebi, D., “Combustion of CH4/H2 mixtures in gas turbines – flame speed and risk of flashback”, International Gas Turbine Congress, Tokyo, November 17-22, 2019

Ebi, D., & Jansohn, P., “Boundary layer flashback limits of hydrogen-methane-air flames in a generic swirl burner at gas turbine relevant conditions”, J. Eng. Gas Turbine and Power, 143(8), 081011 (7 pp.), 2021. https://doi.org/10.1115/1.4049777

Ebi, D., Bombach, R., Jansohn, P., “Swirl flame boundary layer flashback at elevated pressure: Modes of propagation and effect of hydrogen addition”, Proceedings of the Combustion Institute, 38(4), 6345-6353, 2021. https://doi.org/10.1016/j.proci.2020.06.305

13 References

Colin O., F. Ducros, D. Veynante, T. Poinsot, A thickened flame model for large eddy simulations of turbulent premixed combustion, *Physics of Fluids* 12 (7) (2000) 1843-1863.

Donohoe, N., Heufer, A., Metcalfe, W. K., Curran, H. J., Davis, M. L., Mathieu, O., Plichta, D., Morones, A., Petersen, E. L., & Güthe, F. (2014). Ignition delay times, laminar flame speeds, and mechanism validation for natural gas/hydrogen blends at elevated pressures. *Combustion and Flame*, *161*(6), 1432–1443. https://doi.org/10.1016/j.combustflame.2013.12.005

Ebi, D., & Clemens, N. T. (2016). Experimental investigation of upstream flame propagation during boundary layer flashback of swirl flames. *Combustion and Flame*, *168*, 39–52. https://doi.org/10.1016/j.combustflame.2016.03.027

Ebi, D., Ranjan, R., & Clemens, N. T. (2018). Coupling between premixed flame propagation and swirl flow during boundary layer flashback. *Experiments in Fluids*, *59*(7), 109. https://doi.org/10.1007/s00348-018-2563-7

Eichler, C., Flame flashback in wall boundary layers of premixed combustion systems, PhD thesis, Technical University of Munich

Eichler, C., & Sattelmayer, T. (2012). Premixed flame flashback in wall boundary layers studied by long-distance micro-PIV. *Experiments in Fluids*, *52*(2), 347–360. https://doi.org/10.1007/s00348-011-1226-8

Endres, A., & Sattelmayer, T. (2019). Numerical Investigation of Pressure Influence on the Confined Turbulent Boundary Layer Flashback Process. *Fluids*, *4*(3), 146. https://doi.org/10.3390/fluids4030146

ETN Global. (2020). *Hydrogen Gas Turbines*. https://etn.global/wp-content/uploads/2020/01/ETN-Hydrogen-Gas-Turbines-report.pdf

Gicquel, L. Y. M., N. Gourdain, J. F. Boussuge, H. Deniau, G. Staffelbach, P. Wolf, T. Poinsot, High performance parallel computing of flows in complex geometries, Comptes Rendus Mecanique 339 (2), (2011) 104-124.

D. G. Goodwin, R. L. Speth, H. K. Mo_at, B. W. Weber, *Cantera*: An object-oriented software toolkit for chemical kinetics, thermodynamics, and transport processes, 2018. Version 2.4.0

Germano, M., U. Piomelli, P. Moin, W. H. Cabot, A dynamic subgridscale eddy viscosity model, *Phys.Fluids* 3 (7) (1991) 1760-1765.

Gruber, A., Chen, J. H., Valiev, D., & Law, C. K. (2012). Direct numerical simulation of premixed flame boundary layer flashback in turbulent channel flow. *Journal of Fluid Mechanics*, *709*, 516–542. https://doi.org/10.1017/jfm.2012.345

Gruber, A., Kerstein, A. R., Valiev, D., Law, C. K., Kolla, H., & Chen, J. H. (2015). Modeling of mean flame shape during premixed flame flashback in turbulent boundary layers. *Proceedings of the Combustion Institute*, *35*(2), 1485–1492. https://doi.org/10.1016/j.proci.2014.06.073

Hoferichter, V., Hirsch, C., & Sattelmayer, T. (2016). Prediction of Confined Flame Flashback Limits Using Boundary Layer Separation Theory. *Journal of Engineering for Gas Turbines and Power*, *139*(February), 1–10. https://doi.org/10.1115/1.4034237

Hoferichter, V., Hirsch, C., & Sattelmayer, T. (2017). Analytic prediction of unconfined boundary layer flashback limits in premixed hydrogen–air flames. *Combustion Theory and Modelling*, *21*(3), 382–418. https://doi.org/10.1080/13647830.2016.1240832

Ji, C., Wang, D., Yang, J., & Wang, S. (2017). A comprehensive study of light hydrocarbon mechanisms performance in predicting methane/hydrogen/air laminar burning velocities. *International Journal of Hydrogen Energy*, *42*(27), 17260–17274. https://doi.org/10.1016/j.ijhydene.2017.05.203

Kalantari, A., & McDonell, V. (2017). Boundary layer flashback of non-swirling premixed flames: Mechanisms, fundamental research, and recent advances. *Progress in Energy and Combustion Science*, *61*, 249–292. https://doi.org/10.1016/j.pecs.2017.03.001

Li, J., Z. Zhao, A. Kazakov, F. L. Dryer, An updated comprehensive kinetic model of hydrogen combustion, *Int. J. Chem. Kinet.* 36 (10) (2004) 566-575.

Lewis, B., & Elbe, G. von. (1943). Stability and structure of burner flames. *The Journal of Chemical Physics*, *11*(2), 75--97. http://link.aip.org/link/?JCPSA6/11/75/1

Meher-Homji, C. B., Zachary, J., & Bromley, A. F. (2010). Gas turbine fuels - system design, combustion and operability. *Proceedings of the Thirty-Ninth Turbomachinery Symposium*, 155–185.

Metcalfe, W. K., Burke, S. M., Ahmed, S. S., & Curran, H. J. (2013). A hierarchical and comparative kinetic modeling study of C1 - C2 hydrocarbon and oxygenated fuels. *International Journal of Chemical Kinetics*, *45*(10), 638–675. https://doi.org/10.1002/kin.20802

Van Driest, E.R., Turbulent boundary layer in compressible fluids, *J. Aero. Sci.* 18 (3) (1951) 145-160.

Wieneke, B. (2015). PIV uncertainty quantification from correlation statistics. *Measurement Science and Technology*, *26*(7), 074002. https://doi.org/10.1088/0957-0233/26/7/074002